Development and Adjustment of MDOT's Pavement Condition Ratings (PCRs)

by

Anthony Jose Brenes-Calderón

A thesis submitted to the Graduate Faculty of
Auburn University
in partial fulfillment of the
requirements for the Degree of
Master of Science

Auburn, Alabama
December 10, 2022

Keywords: Pavement, PCR, Pavement Management System, Transportation asset management

Approved by

Adriana Vargas-Nordcbeck, Associate Professor of Civil Engineering
Benjamin Bowers, Assistant Professor of Civil Engineering
Carolina Rodezno, Associate Professor of Civil Engineering

ABSTRACT

Pavement condition assessment is a fundamental activity of every pavement management system (PMS). It determines the overall road network condition, as well as possible maintenance and rehabilitation activities (M&R) for restoring pavements' structural and functional capacity. Before determining those required M&R procedures, the overall network condition is reported to upper management and legislature for a specific allocation of the available resources. The Mississippi Department of Transportation (MDOT) still use the pavement condition rating (PCR) for high-level reporting due to their comprehensive interpretation (0- 100 scale, comparable to a school examination).

The current PCR calculation method is based on a point deduction process according to each distress type, severity, and extension. However, multiple changes such as variations in the pavement distresses accounted, multiple vendors in charge of condition assessment activities, and different sections being analyzed have occurred in the past decades. Therefore, MDOT requires a unified and straightforward PCR calculation process that comprises the predominant distresses for each pavement type. Consequently, the previous statement was considered as the main objective of the present study.

PCR models were developed based on a provided database that included multiple pavement sections, their respective distresses, and PCR values from MDOT's biannual pavement network assessment (1995 to 2020). A least squares procedure was used for determining the specific weights of each distress or performance indicator. These weight factors also helped adjust the predicted PCR values to historical PCR trends. Statistical analysis was performed to determine if there was an adequate agreement between predicted and historical PCRs, as well as appropriate

accuracy for the developed models. The main results reveal that there is a strong to very strong agreement between the predicted and historical PCRs. Moreover, the developed models can accurately predict between 65% to 70% of the unseen data. As data become available further calibrations can be performed and models' accuracy can be improved.

ACKNOWLEDGMENTS

I would like to thank and recognize my advisor, Dr. Adriana Vargas-Nordcbeck, for the opportunity, guidance, and mentorship provided during the master's program. Her advice has been a fundamental asset for the continuous improvement of my professional career. Additionally, I would like to recognize my committee members, Dr. Benjamin Bowers and Dr. Carolina Rodezno, for their valuable observations and contributions to this project.

Furthermore, I would like to thank Dr. Leiva and Dr. Castro for their continuous support and advice since the application process to Auburn University. Also, I would like to thank all my friends that have been an essential part of this journey at Auburn University. I am sure that this stage of my life would not have been the same without all of them and the amazing experiences we shared together. Additionally, I would like to thank all the NCAT staff and professors.

Just as importantly, I would like to thank my parents Mr. Jose Alfredo Brenes and Mrs. Paula Calderón for all the support, guidance, and love. As well as all my family members that were part of this process. This goal would not be possible without all your support.

TABLE OF CONTENTS

ABSTRACT 2

ACKNOWLEDGMENTS 4

TABLE OF CONTENTS 5

LIST OF TABLES 8

LIST OF FIGURES 9

LIST OF ABBREVIATIONS 11

CHAPTER 1: INTRODUCTION 12

1.1. BACKGROUND AND PROBLEM STATEMENT 12
1.2. OBJECTIVES 13
1.3. SCOPE 14
1.4. ORGANIZATION OF THESIS 14

CHAPTER 2: LITERATURE REVIEW 16

2.1 INTRODUCTION 16
2.2 PAVEMENT MANAGEMENT SYSTEMS (PMS) 16
2.3 PAVEMENT TYPES 18
2.4 CONDITION DATA (SURVEYED DISTRESSES AND SEVERITY LEVELS) 19
2.4.1 STRUCTURAL CRACKING (FATIGUE CRACKING) 20
2.4.2 NON-STRUCTURAL CRACKING (TRANSVERSE AND LONGITUDINAL) 21
2.4.3 RUTTING 22
2.4.4 POTHOLES 23
2.4.5 SMOOTHNESS 23
2.4.6 FAULTING 24
2.4.7 SPALLING 25
2.4.8 DURABILITY CRACKING (D-CRACKING) 26
2.4.9 PUNCHOUTS 26
2.5. PAVEMENT CONDITION RATING SYSTEMS 28
2.5.1 INDICES DEFINED BASED ON DIRECT PANEL RATINGS 28
2.5.2 INDICES DETERMINED BASED ON UTILITY VALUES 30
2.5.3 INDICES DETERMINED BASED ON DEDUCT VALUES AND WEIGHT FACTORS 31

2.5.4 PAVEMENT CONDITION INDICES USED BY STATES IN THE MDOT LTPP CLIMATIC REGION 35
2.5.5 CALCULATION OF PAVEMENT CONDITION RATING (PCR) USED BY MDOT 38
2.5.6 DECISION TREES FOR MAINTENANCE AND REHABILITATION ACTIVITIES USED BY MDOT 41
2.5. SUMMARY 43

CHAPTER 3: METHODOLOGY 44

3.1 DATA COLLECTION AND DISTRESS IDENTIFICATION PROCESS 44
3.2 DATABASE DESCRIPTION 47
3.3 DISTRESS DENSITIES 49
3.4 INDIVIDUAL DISTRESS-SEVERITY RATING MODELS 52
3.5 PCR CALCULATION PROCESS (WEIGHT FACTORS) 54
3.5.1 DATA SPLITTING METHODS 57
3.6 STATISTICAL INDICATORS (MODEL EVALUATION) 59
3.6.1 COEFFICIENT OF DETERMINATION (R^2) 60
3.6.2 ROOT MEAN SQUARE ERROR (RSME) AND MEAN ABSOLUTE ERROR (MAE) 60
3.6.3 CONCORDANCE CORRELATION COEFFICIENT (CCC) 61
3.6.4 CONFUSION MATRIX 63
3.7 SUMMARY 65

CHAPTER 4: RESULTS 66

4.1 DISTRESS SEVERITY LEVEL RATING MODELS 66
4.1.1 RUTTING INDEX 66
4.1.2 ROUGHNESS “MRI” INDEX 68
4.1.3 FAULTING INDEX 69
4.1.4 LONGITUDINAL AND TRANSVERSE CRACKING INDEX 70
4.1.5 STRUCTURAL CRACKING INDEX 72
4.2 PCR MODELS FOR EACH PAVEMENT TYPE 73
4.2.1 FLEX PAVEMENT PCR MODEL 73
4.2.2 JCP PAVEMENT PCR MODEL 77
4.2.3 COMP PAVEMENT PCR MODEL 79
4.2.4 CRCP PAVEMENT PCR MODEL 81
4.3 MODEL RESIDUALS AND CONFUSION MATRICES 84
4.4 SUMMARY 88

CHAPTER 5: CONCLUSIONS AND RECOMMENDATIONS 89

5.1 CONCLUSIONS 89
5.2 RECOMMENDATIONS 90

REFERENCES 91

APPENDIX 1: ANALYSIS OF EXISTING DATABASE 97

LIST OF TABLES

Table 1. Pavement Condition Indices Southern Region Agencies (Papagiannakis 2009; Bektas 2014). 36
Table 2. Predominant Distresses on PCR calculation (Pathway Services 2016). 38
Table 3. Deduct points example for flexible pavement 40
Table 4. Thresholds for MDOT decision trees. 42
Table 5. Model evaluation using randomly splitting method (training and validation). 58
Table 6. Training and validation average errors for randomly splitting method. 59
Table 7.Training and validation error for time-based splitting method 59
Table 8. Rutting index model parameters. 67
Table 9. MRI index model parameters. 69
Table 10. Faulting index model parameters. 70
Table 11. Non-structural cracking index model parameters. 71
Table 12. Structural cracking index model parameters. 73
Table 13. Weight factors for FLEX pavements. 75
Table 14. Average of statistical indicators for FLEX pavement model. 76
Table 15. Weight factors for JCP pavements. 78
Table 16. Average of statistical indicators for JCP pavement model. 79
Table 17. Weight factors for COMP pavements. 80
Table 18. Average of statistical indicators for COMP pavement model. 81
Table 19. Weight factors for CRCP pavements. 82
Table 20. Average of statistical indicators for CRCP pavement model. 83
Table 21. Average percentage of PCR residuals within practical limits. 85
Table 22. Average calculated model accuracy. 87

LIST OF FIGURES

Figure 1. PMS Process (Vargas 2021). 18
Figure 2. Alligator Cracking and Severity Levels Identification (Pathway Services Inc 2016)... 21
Figure 3. Transverse Cracking and Severity Levels Identification (Pathway Services Inc 2016). 22
Figure 4. Smoothness specifications for pavements in the United States (Merritt et al. 2015).... 24
Figure 5. Faulting mechanism (Ayers et al. 2018)..... 25
Figure 6. Punchout development mechanism (Jeon et al. 2021). 27
Figure 7. The general shape of utility curves (Menendez 2014). 31
Figure 8. Typical deduct value curve (Shahnazari et al. 2012). 33
Figure 9. Development of deduct value curves (City and County Pavement Improvement Center 2021). 34
Figure 10. Climatic zones defined by the LTPP (Zhang et al. 2015). 35
Figure 11. MDOT's PCR quantification process. 41
Figure 12. PCR classification used by MDOT (MDOT 2022) 42
Figure 13. Lane Breakdown for Distress Identification. (Pathway Services Inc 2016). 46
Figure 14. Comparison of PCR with all distresses and PCR without potholes and patching (Chowdari 2019). 47
Figure 15. Comparison of PCR with all distresses and PCR without less frequent distresses. 49
Figure 16. Structural cracking density determination. 50
Figure 17. Density definition for linear cracking. 51
Figure 18. MDOT proposed scores for MRI values. 52
Figure 19. Log-logistic sigmoidal curve (Adapted from: Onofri (2019)). 54
Figure 20. PCR calculation sequence, FLEX example. 55
Figure 21. PCR general calculation flowchart. 56
Figure 22. Data splitting methods. 58
Figure 23. CCC vs Pearson Correlation Coefficient (Gossman 2020). 62
Figure 24. Confusion matrix for PCI model (Piryonesi and El-Diraby 2018)..... 64
Figure 25. Rutting proposed indices and fitted model. 67
Figure 26. Roughness proposed indices and fitted model. 68

Figure 27. Faulting proposed indices and fitted model. 70
Figure 28. Non-structural cracking index model. 71
Figure 29. Structural cracking index model. 72
Figure 30. Analyzed flexible pavement sections. 74
Figure 31. FLEX PCR comparison for validation and training datasets. 75
Figure 32. Analyzed jointed concrete pavement sections. 77
Figure 33. JCP PCR comparison for validation and training datasets. 78
Figure 34. Analyzed composite pavement sections. 79
Figure 35. COMP PCR comparison for validation and training datasets. 80
Figure 36. Analyzed continuously reinforced concrete pavement sections. 82
Figure 37. CRCP PCR comparison for validation and training datasets. 83
Figure 38. Cumulative Residual Distribution. 85
Figure 39. Confusion matrix for each pavement model. 87

LIST OF ABBREVIATIONS

Abbreviation	Definition
AASHTO	American Association of Highway and Transportation Officials
AC	Asphalt Concrete
ASTM	American Society for Testing and Materials
CCC	Concordance Correlation Coefficient
COMP	Composite Pavement
CRCP	Continuously Reinforced Concrete Pavement
CS	Condition Score
DS	Distress Score
FHWA	Federal Highway Administration
FLEX	Flexible Pavements
HMA	Hot Mix Asphalt
IRI	International Roughness Index
JCP	Jointed Concrete Pavement
JPCP	Jointend Plain Concrete Pavement
JRCP	Jointed Reinforced Concrete Pavement
LTPP	Long-Term Pavement Performance
M&R	Maintenance and Rehabilitation
MAE	Mean Absolute Error
MDOT	Mississippi Department of Transportation
MRI	Mean Ride Index
PCI	Pavement Condition Index
PCR	Pavement Condition Rating
PMS	Pavement Management System
RSME	Root Mean Squared Error
SI	International System

CHAPTER 1: INTRODUCTION

1.1. BACKGROUND AND PROBLEM STATEMENT

Pavement condition assessment is a crucial activity performed within any pavement management system, in which data is continuously collected, processed, and analyzed to determine the condition of the pavement network being evaluated. According to Pierce et al. (2013), pavement condition rating protocols should clearly describe the distresses accounted, severity levels, rating methods, and the procedures implemented to compute the condition values, to prevent any incomprehension or inconsistencies that can negatively impact the effectiveness of the data that the agency receives.

The Mississippi Department of Transportation (MDOT) has been continuously collecting pavement management system (PMS) condition data, using contract vendors approximately every two years since 1991. Pavement condition ratings (PCRs) were initially developed for MDOT during the early 1990s by the University of Mississippi (George 2000). Starting with the 2006 survey, MDOT implemented a new in-house-developed and density-based PCR system. The PCR was utilized for maintenance prioritization up until 2011 when MDOT started using decision trees for repair recommendations. Nevertheless, PCRs are still used for high-level reporting to upper management and the legislature due to their comprehensive interpretation (0- 100 scale, comparable to a school examination).

The current PCR calculation process is based on a point deduction process according to each distress type, severity, and extension. Additionally, deduct values for Mean Roughness Index (MRI), rutting, and faulting are also included. These deducted points are finally added up and put

into equations based on the pavement type (asphalt, composite, jointed concrete, and continuously reinforced concrete) to obtain the resultant PCR.

Over the years, technology has changed, and MDOT has not always contracted with the same vendors. For this reason, there have been multiple variations in the distress assessment process. To cite some instances:

- Change from three-laser-point rut collection to scanning laser (over 1200 transverse points) in approximately 2008.
- Change from the collection of two 500 ft samples per mile, approximately 20% coverage, to 100% collection in 2010.
- Change from human rating and digitizing to fully automated distress detection with human quality assurance with the 2010 condition survey.
- The continuous improvement in camera resolution, allows a broader distress detection variety.

Added to the listed technology changes, there have been other obstacles to a precise PCR calculation procedure and consistent reporting, such as the imperfect nature of automated distress detection, multiple vendors and proprietary technology, rater subjectivity of human-rated distresses, removed distresses from PCR calculation method, and time challenge for quality assurance of the data collected (data is always at least several months old before it is ready for general consumption). Therefore, MDOT has been looking for an alternative procedure for calculating PCRs, based on the predominant distresses for each pavement type, and adjusted to historical observations to prevent significant differences in the actual network condition.

1.2. OBJECTIVES

Due to the need for a comprehensive PCR system, the objectives of this thesis were:

1. Generate a PCR index for evaluating the MDOT's pavement network, based on the predominant distresses for each pavement type.
2. Develop individual rating indices for each distress and pavement type, according to MDOT's recommendations and PMS condition data.
3. Determine the contribution of each distress type on the calculated PCR for each pavement type.
4. Evaluate the concordance and correlation of the proposed PCR system with historical PCR observations.

1.3. SCOPE

To accomplish the objectives mentioned above, this study initiated with a literature review of existing pavement rating systems and the variables involved in the process. According to the findings from the literature review and based on a PMS condition historical database (1995 - 2020) provided by MDOT, a research plan was developed. This plan incorporated the extraction and processing of the raw data, the development of individual distress-severity rating models using non-linear regression procedures, and the creation of PCR curves using weighting factors techniques that quantified the contribution of the predominant distresses on each pavement type. Finally, the agreement between the predicted PCR and historical observations was assessed through statistical analysis.

1.4. ORGANIZATION OF THESIS

The main body of the present document is subdivided into four chapters, as follows:

- Chapter 2. Literature Review: This section comprises a literature review of different scoring methods for assessing the actual pavement condition. Additionally, it defines

fundamental components of a pavement management system that are included in a condition rating procedure such as predominant pavement distresses, pavement types, data collection, and condition analysis.

- Chapter 3. Methodology: This chapter presents the different methods used to create and evaluate the new PCR system, such as data splitting methods, description of the statistic parameters used for the agreement and concordance assessment, description of individual distress rating models and weight factors. Also, it provides a brief explanation of the main database components.
- Chapter 4. Results: This section comprises the generated distress rating models, weight factors and the obtained statistics indicators for each pavement type, along with a discussion of the main findings.
- Chapter 5. Conclusions and recommendations: This chapter summarizes the main conclusions and recommendations regarding the PCR system for MDOT.

CHAPTER 2: LITERATURE REVIEW

2.1 INTRODUCTION

Pavement condition assessment is a fundamental and recurring activity of all departments of transportation (DOTs) and administrations. Surveys are performed to determine the structural and functional elements provided by a pavement structure. For this reason, various of indices or rating systems have been developed, with the main objective of expressing the actual pavement condition according to a defined scale.

Pavement condition indices are an accumulation of several distresses that can be generated by multiple agents such as environmental conditions, loading scenarios, structure aging, or a combination of these factors (Gharaibeh et al. 2010). Consequently, these indices are highly dependent on the pavement type, distress nature, and agency needs (selected distress types to be included in the index). Additionally, other pavement characteristics relevant to administrations and users might be also utilized as indices, as is the case for pavement roughness (Fatih Bektas et al. 2014). These different pavement measurements are commonly grouped into a single index that attempts to characterize the structure's overall condition. Therefore, the condition assessment and compilation of all this information are crucial activities for every PMS (Sarsam 2016).

2.2 PAVEMENT MANAGEMENT SYSTEMS (PMS)

In previous decades, pavements were maintained but not managed; pavement engineers' experience determined the selection of maintenance and rehabilitation activities, despite life-cycle cost scenarios or prioritization concepts (Shahin 2005). Consequently, backlogs in resources and

the need for major rehabilitation activities were experienced, which prompted the introduction of the PMS concept in the late 1970s (Kulkarni and Miller 2002). Since that period, this concept has been widely adopted and studied in the pavement engineering field. For instance, in 1991, the FHWA recognized the value of the PMS at a national level by including mandatory policies requiring states to have an operational pavement management system for principal arterials (Finn 1998).

Multiple definitions have been given to the PMS concept. Nevertheless, all of them agree that it is a systematic group of procedures for collecting, analyzing, maintaining, and reporting pavement data, to support decision-makers (pavement managers), in selecting optimum strategies for maintaining pavements at an adequate serviceable level (Haas et al. 1994; Vitillo 2009).

A PMS comprises multiple elements or functions that are put together to achieve the objective. According to Vargas (2021) and Shahin (2005), the process starts with data collection. This process comprises different survey methods, road network characteristics, and multiple pavement distresses. The second element is the pavement condition assessment, in which the administrators rate pavements according to defined scales. Third, future performance is predicted using performance models, which typically involve future traffic parameters and actual pavement conditions. Moreover, maintenance and rehabilitation (M&R) activities are listed and budget scenarios are defined according to available resources. Then life cycle costs analysis, possibly combined with non-monetary factors such as contractor's availability or life cycle assessments, is performed. Finally, a scientifically grounded decision is taken, and M&R activities are executed. Performance should be continuously monitored for entering again into the cyclic process. Figure 2 illustrates the general process and functions developed by a PMS.

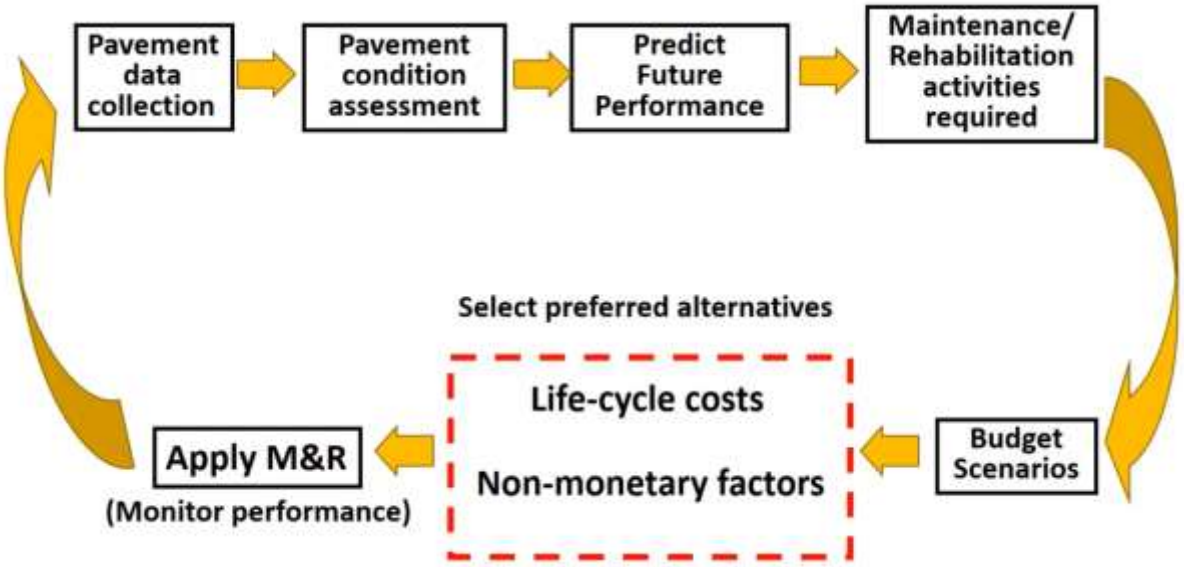

Figure 1. PMS Process (Vargas 2021).

2.3 PAVEMENT TYPES

MDOT has collected information for different pavement types along their road network. For a comprehensive data analysis, pavements have been grouped into four main types (Pathway Services Inc 2016), as follows:

1. Flexible Pavements (FLEX): flexible pavements are characterized by a multi-layer structure, in which high-quality materials are placed on the top layers where the stress concentration is higher (Huang 2004). Therefore, a typical flexible pavement cross-section consists of an asphalt concrete (AC) mixture surface course, granular base, and subbase, that have been placed over a treated or compacted subgrade
2. Composite Pavements (COMP): composite pavements consist of a layered system in which an asphalt surface course is placed over a rigid layer, usually a previous concrete pavement structure. In this type of pavement, the stiffness of the base layer is greater than that of the surface layer (flexible layer) (Flintsch et al. 2008).

3. Jointed Concrete Pavements (JCP): jointed concrete pavements are distinguished by a surface layer made-up of adjacent slabs separated by transverse and longitudinal joints. These concrete slabs are typically placed over a granular subbase or directly over a compacted subgrade. Depending on the presence of dowels, steel mesh, and slab length, JCP can be categorized as Jointed Plain Concrete Pavements (JPCP) or Jointed Reinforced Concrete Pavement (JRCP) (Huang 2004). Despite the differences between pavement types, MDOT has included them in the same category for the condition assessment process (Pathway Services Inc 2016).
4. Continuously Reinforced Concrete Pavements (CRCP): continuously reinforced concrete pavements are characterized by the presence of continuous longitudinal steel reinforcement and the absence of transverse joints, excluding the ones required for the end-of-day header joints (Roesler et al. 2016). This type of pavement is intentionally designed to crack; however, steel is intended to hold cracks together and prevent any future punchouts or spalling distress (Concrete Reinforcing Steel Institute 2001).

2.4 CONDITION DATA (SURVEYED DISTRESSES AND SEVERITY LEVELS)

Pavements are exposed to multiple agents that accelerate their distress development process. Repetitive traffic loads, moisture action, freeze and thaw cycles, and ultraviolet (UV) radiation are some of these agents. In addition to the environmental factors, pavement type and

structure configuration play a crucial role in the deterioration process, due to differences in structural capacity and strength (Llopis-Castelló et al. 2020).

Due to the absence of a uniform distress identification procedure, administrations have developed multiple methods for quantifying and classifying pavement distresses and their respective severity levels. Nevertheless, the Long-Term Pavement Performance (LTPP) program, established by the Federal Highway Administration (FHWA), has developed a distress identification manual that aims to improve communications within the pavement community by adopting more consistent definitions (Miller and Bellinger 2014). MDOT has adopted some of these definitions for several of its pavement distresses.

Administrations usually define their predominant pavement distresses according to the observed frequency, the given importance, and the pavement types that make up the network (Shahin 2005). Therefore, MDOT has created a list of multiple pavement distresses conceptualized as “predominant”, that has been modified over the past years. The following subsections define each of the distresses and their respective severity levels.

2.4.1 STRUCTURAL CRACKING (FATIGUE CRACKING)

Structural cracking also referred to as fatigue cracking, is one of the primary distresses in asphalt pavements. It is mainly caused by repetitive traffic loading and an insufficient asphalt layer thickness (Norouzi and Kim 2017). The combination of these factors generates a higher tensile stress concentration at the bottom of the AC, which leads to a crack propagation from the bottom of the AC to the surface (for this reason is also known as “bottom-up cracking”) (Mackiewicz 2018).

MDOT utilizes the LTPP procedures to categorize this type of cracking. This is mainly identified by the interconnection of multiple-sided, sharp-angled pieces, usually less than 1ft on

the longest side, that create an “alligator” pattern on the wheel paths (John Miller and William Bellinger 2014). The same authors stated that three different severity levels can be associated with this flexible pavement distress, as follows:

Low Severity: a group of cracks not completely interconnected without spalling or pumping traces.

Moderate Severity: a group of interconnected cracks creating a complete pattern. Some of the cracks can start experiencing spalling.

High Severity: spalled and interconnected cracks that create a complete pattern on the wheel path. Pumping of fines from the cracks can indicate this severity level.

Figure 2, illustrates the three fatigue cracking severity levels from the automated distress identification perspective.

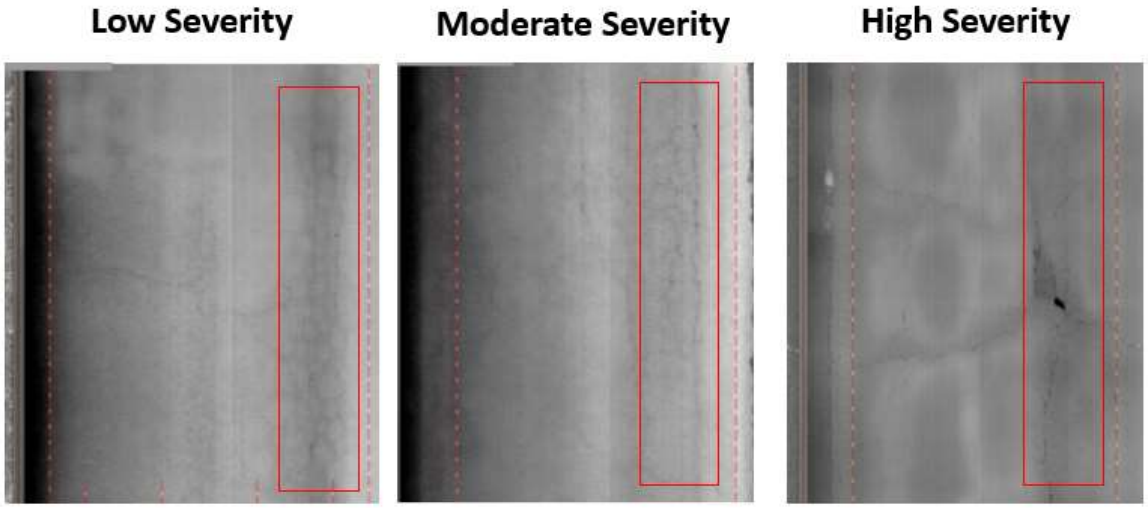

Figure 2. Alligator Cracking and Severity Levels Identification (Pathway Services Inc 2016).

2.4.2 NON-STRUCTURAL CRACKING (TRANSVERSE AND LONGITUDINAL)

Non-structural cracking is a pavement distress mainly caused by non load-related agents in both flexible and rigid pavements. It is typically divided into two main categories depending on the crack orientation across the pavement centerline (longitudinal and transverse cracking).

Longitudinal cracking (cracks parallel to the pavement centerline), is mainly produced by inadequately constructed joints or shrinkage of the AC layer. Meanwhile, transverse cracking (cracks perpendicular to the pavement centerline), is produced by the crack reflection from underlying structures or shrinkage of the AC layer in flexible pavements (Kumar and Gupta 2010).

MDOT has implemented the LTPP Distress Identification Manual definitions to categorize this distress. It includes three severity levels (low, moderate, and high), that mainly depend on the crack width, pavement type, and the interconnection between cracks (Miller and Bellinger 2014). Therefore, with the automated distress identification procedures, the combination of crack depth, width, texture, and pixels has been crucial when determining severity variations (Pathway Services Inc 2016). Figure 3 illustrates the identification of different severity transverse cracks.

2.4.3 RUTTING

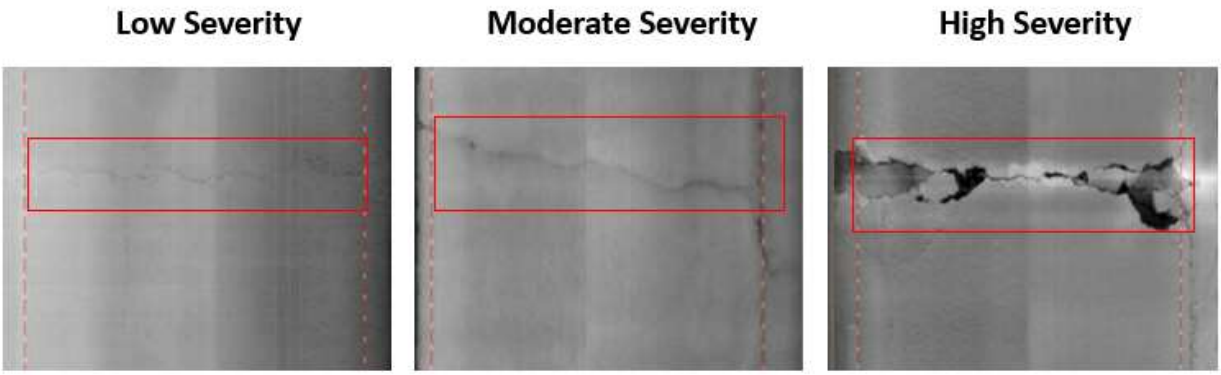

Figure 3. Transverse Cracking and Severity Levels Identification (Pathway Services Inc 2016).

Rutting has been a typical flexible and composite pavement distress, defined as a measurable longitudinal surface depression in the wheel path (Miller and Bellinger 2014; Simpson 1999). This common distress can be caused by multiple factors, such as inadequate compaction during construction (significant decrease in air voids by the effects of repeated axle loads and high temperature), permanent deformation of underlying layers (known as structural rutting), inadequate aggregate gradation in the asphalt mixture (unbalanced fines portion or insufficient

aggregate strength), or deficient asphalt layer stiffness due to inadequate binder proportion or grade selection (Xu and Huang 2012).

In relation to the LTPP Distress Identification manual, severity levels can be defined based on the rut depth, therefore measurements taken can be categorized according to their magnitude (Miller and Bellinger 2014). As an instance, MDOT has used this distress as part of their decision trees, explained in further sections.

2.4.4 POTHOLES

According to Miller and Bellinger (2014), potholes are pavement distresses characterized by a bowl-shaped depression in the pavement structure surface. They caused mainly by the presence of two agents, traffic loading, and moisture. Nevertheless, other common causes have been studied such as lack of bonding between the surface layer and the base course, segregation of the asphalt mixture during laying (increasing permeability due to a reduction of fines portion), presence of weak spots in any of the pavement layers during constructions (Yadav and Anusha 2018).

Even though the LTPP Distress Identification manual categorizes the severity levels according to the pothole depth, MDOT has decided to categorize them according to their respective area (Low: 0.5 ft^2 to 1 ft^2, Moderate: 1 ft^2 to 2 ft^2, High: greater than 2 ft^2), (Pathway Services Inc 2016).

2.4.5 SMOOTHNESS

Pavement smoothness is typically associated with measuring the level of comfort experienced by users while driving over a pavement surface (Federal Highway Administration 2016). As a standardized definition, it has been interchangeably referred to as roughness, and defined as an expression of the deviation of a surface from a true planar surface (American Society

of Testing Materials (ASTM) 2020a). Therefore, it is a crucial parameter for pavement longitudinal profile characterization.

Multiple devices have been implemented for measuring pavement smoothness, at the network level agencies have utilized high-speed inertial profilers equipped with laser sensors that record actual elevation measurements along the pavement (Federal Highway Administration 2016). This equipment not only allows data collection at highway speeds, but also mitigates lane closures from smoothness assessment activities.

Despite the existence of numerous indices to report pavement smoothness, the International Roughness Index (IRI) has been the predominant indicator of smoothness specifications in the United States, as shown in Figure 4. IRI is defined as an index computed from a longitudinal profile measurement using a quarter-car simulation at a simulation speed of 50 mph (ASTM 2020). Specifically, the IRI is based on a single profile measure in one of the wheelpaths (commonly the right wheelpath) (FHWA 2016). Nevertheless, agencies such as MDOT gather the IRI values from both wheelpaths and average them, which results in a statistic indicator known as the Mean Roughness Index (MRI) (Merritt et al. 2015).

Asphalt Pavements **Concrete Pavements**

Note: IRI (International Roughness Index), PrI (Profile Index), RN (Ride Number), and N/A (Not available).

Figure 4. Smoothness specifications for pavements in the United States (Merritt et al. 2015).

2.4.6 FAULTING

Faulting is a pavement distress characteristic of jointed concrete pavements. It has been defined as a difference in elevation across a joint or crack (Miller and Bellinger 2014). This pavement distress is mainly caused by the combination of different agents. Consequently, several authors have described the faulting mechanism as a multiple step process. First, the presence of an erodible material and moisture on the base layer, creates an unstable support. Then a poor load transfer between adjacent slabs occurs due to damaged dowels or inadequate aggregate interlock. Finally, heavy loading (truck traffic) accelerates transversal displacements between slabs. (Ayers et al. 2018; Huang 2004; DeSantis et al. 2020). Figure 5 illustrates the described process.

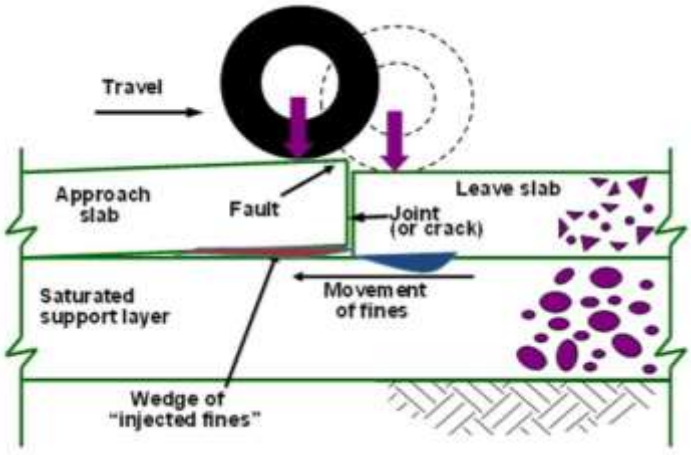

Figure 5. Faulting mechanism (Ayers et al. 2018)

According to Miller and Bellinger (2014), faulting is measured as the elevation difference between the departure slab and the approach slab. Additionally, severity levels can be defined according to the faulting magnitude. Therefore, measurements taken can be grouped, as for roughness and rutting in asphalt pavements.

2.4.7 SPALLING

Spalling is a concrete pavement distress distinguished by the cracking or breaking of the slab edge within 1 ft from the face of either the transverse or longitudinal joint (Miller and

Bellinger 2014). Multiple physical and chemical causes have been associated with this distress; some cases include misalignment of dowels, infiltration of materials into inadequately sealed joints, curling, and warping movements, and freeze and thaw damage (Ayers et al. 2018). In addition, on CRCP pavements spalling has been related to bond failure between the surface of coarse aggregates and the surrounding cement paste (Choi et al. 2020).

MDOT has adopted the severity levels included in the LTPP Distress Identification Manual, in which spalling is categorized according to its width (low severity: less than 3 in, moderate severity: between 3 and 6 in, and high severity: greater than 6 in) (Pathway Services Inc 2016).

2.4.8 DURABILITY CRACKING (D-CRACKING)

D-cracking is a concrete pavement distress distinguished by the formation of closely spaced and hairline-shaped cracks on the intersections between transverse and edge joints (Miller and Bellinger 2014). This distress is mainly caused by the presence of susceptible aggregates to freeze and thaw cycles (fracture or dilate), resulting in cracking of the surrounding mortar (Ayers et al. 2018). Therefore, it can be stated that this cracking is mostly a material-related distress.

The different severity levels for this distress have been defined by the guidelines described in the LTPP Distress Identification Manual (low severity: “D” cracks are tight, with no missing pieces; moderate severity: “D” cracks are well-defined, and some small pieces are missing, and high severity: “D” cracking has a clear-developed pattern, with substantial amount of pieces missing) (Pathway Services Inc 2016).

2.4.9 PUNCHOUTS

Punchouts are localized pavement distresses originated on CRCP. They are characterized by an area enclosed by two closely spaced transverse cracks and a longitudinal joint or the

pavement edge (Miller and Bellinger 2014). Jeon et al. (2021) explained the punchout development mechanism in four primary steps. First, transverse cracks are narrowly spaced (2 ft or less). Second, load transfer efficiency is reduced due to deficient aggregate interlock from excessive crack opening and heavy loading. Third, loss of support along the pavement edge is experienced due to base erosion. Finally, temperature gradients and repetitive heavy loading, magnify the bending stresses that lead to a longitudinal cracking formation and punchout definition. Figure 6 illustrates the previously described process.

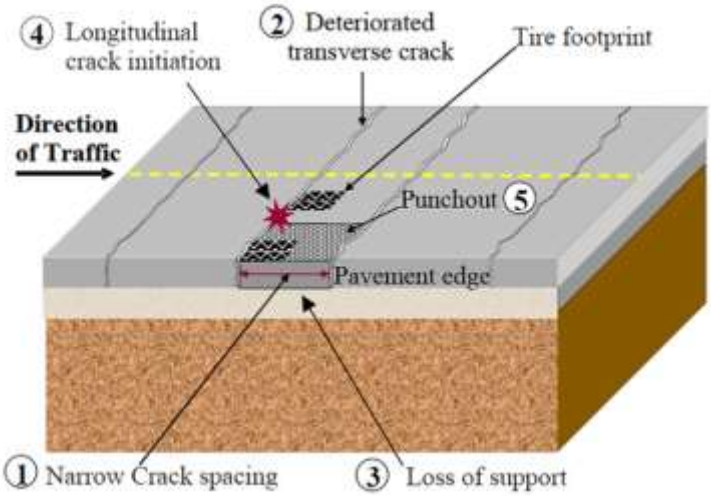

Figure 6. Punchout development mechanism (Jeon et al. 2021).

MDOT implemented the severity levels included in the LTPP Distress Identification Manual, in which punchouts are categorized according to the width of the longitudinal and transverse crack, and the presence of faulting (low severity: less than 3 in; moderate severity: between 3 and 6 in wide, with some spalling and faulting; and high severity: greater than 6 in wide, with clear spalling and faulting) (Pathway Services Inc 2016). In addition, punchouts have been manually analyzed and rated.

2.5. PAVEMENT CONDITION RATING SYSTEMS

The pavement condition rating refers to a score that determines the overall performance of a specific pavement section being analyzed, based on different measurements such as roughness, skid resistance, and deflection, among others obtained during the data collection process (Attoh-Okine and Adarkwa 2013). Therefore, the systematic procedures or rating scales used to determine that score have been interchangeably known as pavement condition rating systems or pavement condition indices.

The described indices not only allow administrations to classify and compare their assets but also, provide pavement managers with valuable information to control and monitor the assets throughout their service life. Additionally, these indicators are intended to be ranked for recommending and prioritizing maintenance and rehabilitation activities. For instance, Papagiannakis et al. (2009) stated that condition ratings enable DOTs and all stakeholders to estimate the maintenance and rehabilitation procedures required, due to their ability to reflect the actual pavement condition.

As already explained, the pavement rating system opted by an agency highly depends on the agency's resources and its ability to address pavement issues commonly experienced in the region. Nevertheless, the development of an index capable of representing the overall pavement condition and combining different characteristics such as distress types, severity levels, distress densities, or extensions into a single value has been a challenge (Gharaibeh et al. 2010). Therefore, many efforts have been made to define those rating systems, where three main methods have been utilized (direct panel rating, utility functions, deduct values and weighting factors) (Bektas et al. 2014). The following subsections describe each of the listed methods.

2.5.1 INDICES DEFINED BASED ON DIRECT PANEL RATINGS

This index methodology is characterized by the presence of a panel of raters or professionals that drive over the pavement sections and rate them implementing a numeric scale or verbal descriptions such as good, fair, and poor (Gharaibeh et al. 2010). Since the given scores are mainly based on observations, without direct measurements, these indices have also been known as subjective or estimated indices (Attoh-Okine and Adarkwa 2013; Gharaibeh et al. 2010).

Subjective indices were the first procedures for rating pavements in the United States. Panel ratings date back to the 1950s, when the Present Serviceability Rating (PSR) (0 to 5 scale created to rate pavement sections subjectively) was developed by the American Association of State Highway and Transportation Officials (AASTHO) in Ottawa, Illinois (Carey and Irick 1960).

Since the first use of panel ratings, multiple procedures have been developed, to cite an instance, the Pavement Surface Evaluation and Rating (PASER). PASER is a rating method based on multiple distress descriptions and pictures used by raters to assess and categorize overall pavement condition on a 1 to 10 scale (1 corresponding to a failed condition and 10 to an excellent condition) (Wolters et al. 2011). Another similar panel rating is the Condition Rating Survey (CRS). CRS has been used by the Illinois Department of Transportation, and it includes several images and descriptions that help inspectors to rate pavements on a 1.0 to 9.0 scale (1 corresponds to a total failure, and 9 to a newly constructed pavement) (Hasan Ozer et al. 2018).

Even though panel ratings are simple and easy to present to roadway users, they are inherently subjective. They do not provide enough engineering data that can be used to identify effective repair strategies (Gharaibeh et al. 2010). Therefore, different computational and mathematical models have been developed for the pavement rating process, as explained in further subsections.

2.5.2 INDICES DETERMINED BASED ON UTILITY VALUES

The utility value method was primarily introduced by the Texas Department of Transportation in the late 1980s and it includes two main pavement performance indices (indicators of functional and structural characteristics, Condition Score (CS) and Distress Score (DS), respectively) (Stampley et al. 1995). According to Bektas et al. (2014), the DS is an index that considers several distresses depending on the pavement structure type, according to a 1 to 100 scale. Meanwhile, CS incorporates the DS and a roughness indicator into a 1 to 100 scale; Equation 1 and Equation 2 are utilized to quantify both indices.

$$DS = 100\ x \prod_{i=i}^{n} U_i \qquad \text{Equation 1}$$

$$CS = DS\ x\ U_{Ride} \qquad \text{Equation 2}$$

Where DS: distress score; U_i: utility values for each distress and pavement type; CS: condition score; U_{Ride}: ride utility.

According to Menendez (2014), an utility value can be defined as the value of the service (either structural or functional) provided by a pavement structure with a certain damage level. In addition, utility values ranging from 0.0001 to 1, corresponding from poor condition to perfect condition. Utility values are calculated from typical sigmoidal "utility curves", defined by the respective agency for each pavement and distress type (Texas Department of Transportation 2010). Figure 7 illustrates a typical utility curve.

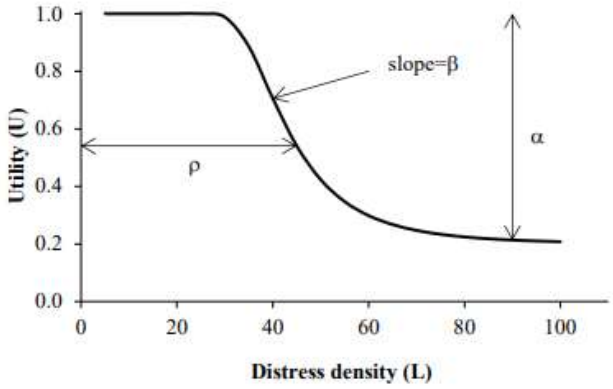

Figure 7. The general shape of utility curves (Menendez 2014).

As shown in Figure 7, three main parameters constitute the sigmodal model implemented by Texas DOT. According to Stampley et al. (1995), "β_i" is the parameter that controls how steeply utility is lost in the middle of the curve, "α_i" is the factor that controls the maximum utility loss that the pavement can experience, also known as an asymptotic parameter, and "ρ_i", known as the prolongation parameter, rules how long the utility curve will last above a certain level. Finally, the distress density "L_i" (i.e. percentage of area cracked, IRI) is the essential input to calculate the utility value (U_i). The typical utility model is presented in Equation 3 (Menendez 2014).

$$U_i = \begin{cases} 1.0 & when\ L_i = 0 \\ 1 - \alpha_i e^{-\left(\frac{\rho_i}{L_i}\right)^{\beta_i}} & when\ L_i > 0 \end{cases} \qquad \text{Equation 3}$$

2.5.3 INDICES DETERMINED BASED ON DEDUCT VALUES AND WEIGHT FACTORS

The deduct values procedure encapsulates the effect of several distress types, severities, extents, and ride quality, on the total score through deduct values (Bektas et al. 2014). Therefore, it differentiates from utility curve procedures by not treating ride quality as an independent

parameter. According to Bektas (2014), the general mathematical model for calculating a determinate pavement condition index (PC) using deduct value procedures is presented in Equation 4.

$$PC = PC_{MAX} - \sum_{i=1}^{n} (a_i \; x \; d_i) \qquad \text{Equation 4}$$

Where PC_{MAX} refers to the maximum score possible, a_i represents the deduct values for each distress type and severity level, and d_i denotes the adjustments or weight factors for each distress type or roughness indicator.

The development of these indices date back to the late 1970s, when the Pavement Condition Index (PCI) was established by the U.S. Army Corps of Engineers (Shahin and Kohn 1979). According to Shahin (2005), PCI is a numerical index that ranges from 0 "failed pavement" to 100 "perfect condition pavement", and it is calculated using the results of a visual condition survey in which distress type, severity, and quantity are registered. This pavement condition index has been widely implemented by multiple agencies, and it has been standardized by the American Society for Testing and Materials (ASTM) into the ASTM 6433, Standard Practice for Roads and Parking Lots Pavement Condition Index Surveys. A brief description of the PCI calculation process can be summarized by the following steps (ASTM 2020b; City and County Pavement Improvement Center 2021):

1. A condition survey should be performed on a representative pavement section. Distress types, extensions and severities should be registered.

2. Deduct values are defined, using the deduct value curves for each distress type and severity presented on the ASTM D-6433 standard. According to Shahnazari et al. (2012), a typical pavement deduct value curve with the respective severity levels is shown in Figure 8.

Figure 8. Typical deduct value curve (Shahnazari et al. 2012).

3. All the deduct values calculated in the previous step (quantified from each distress type and severity) should be added.
4. A correction curve is utilized to adjust the total deduct value for the number of distresses observed to get a corrected deduct value.
5. Finally, the final PCI is calculated as the difference between 100 (maximum PCI possible) and the corrected deduct value from step 4.

The deduct value definition is a fundamental component of this calculation process. According to the City and County Pavement Improvement Center (2021), multiple surveyors subjectively rated distresses (types, severities and extents) during the PCI development process using a 1 to 100 scale. Severities (low, medium and high) were rated according to the surveyors'

opinions, and extent values were defined according to the pavement section's surface area where the distresses were located. All ratings were averaged and used to define the deduct value curves, as shown in Figure 9.

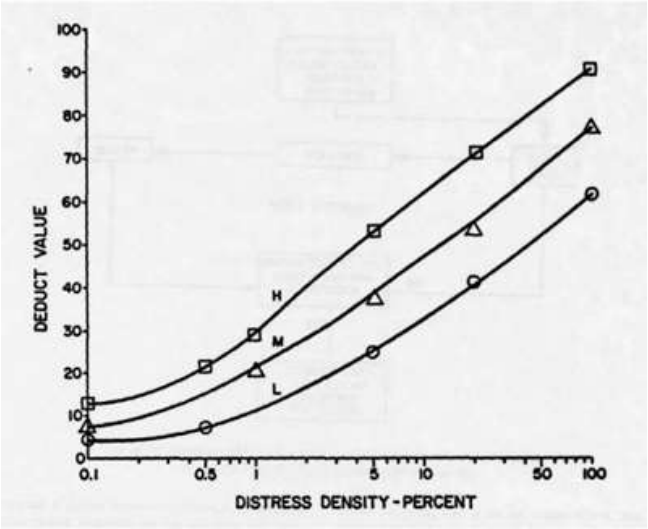

Figure 9. Development of deduct value curves (City and County Pavement Improvement Center 2021).

Since the definition of the deduct value curves has involved subjective components, agencies have implemented different approaches to create their own curves. According to Shahin (2005), the ratio to which a given pavement distress is detrimental to pavement performance is a function of both the extent and the severity of that specific distress. Specifically, deduct values are related to that detrimental effect and typically follow a non-linear trend (absence of a one-to-one relation between distress frequency/severity and the deduct values assigned) (McGhee 2002). Therefore, different studies have implemented non-linear regressions as polynomial or sigmoidal curves to create their own deduct values or scoring system, which sometimes require adjustments by committee reviewers to match the desired indices (Elhadidy et al. 2021; K McGhee 2002; Wu 2015).

2.5.4 PAVEMENT CONDITION INDICES USED BY STATES IN THE MDOT LTPP CLIMATIC REGION

Pavement durability is not only affected by the presence of traffic loadings, pavement characteristics and subgrade properties, but also by the multiple environmental conditions that pavement structures are exposed to, such as moisture and temperature (Tamrakar 2019). Therefore, to account for similar conditions that could lead to similar pavement distresses (fundamental components of pavement condition rating systems), a compilation of the pavement condition indices used by the states on the Wet No Freeze LTPP region was performed. **Error! R eference source not found.** illustrates the region location and Table 1 summarizes the information about the pavement condition rating system implemented in each state.

Figure 10. Climatic zones defined by the LTPP (Zhang et al. 2015).

Table 1. Pavement Condition Indices Southern Region Agencies (Papagiannakis 2009; Bektas 2014).

State	Distresses Collected	Pavement Condition Index
Alabama	Cracking, patching, roughness, rutting, raveling.	Pavement Condition Rating (PCR) scale between 0 and 100. Additionally, a regression model is used to combine all the analyzed distresses.
Arkansas	Roughness, rutting, faulting, and cracking.	Flexible pavements are rated based on ride quality. Meanwhile, concrete pavements involve ride quality and defects.
Florida	Rutting, cracking, roughness (IRI), raveling.	Three or two individual indices are calculated depending on pavement type. Ride rating (quantified with Ride Number, based on IRI), Defect Rating (based on distress just for rigid pavements) or Rut Rating and Crack rating (based on cracking rut depth, respectively and just for flexible pavements). The lowest of the two or three indices is taken as the PCR.
Georgia	Several cracking types depending on pavement type, roughness (IRI), punch-outs, faulting.	In-house developed system to categorize pavements for maintenance and rehabilitation activities, Pavement Condition Evaluation System (PACES).
Louisiana	Rutting depth, cracking and faulting.	Louisiana DOT requires data collection consultants to calculate PSR using a combination of collected distresses (0 to 5 scale) (Louisiana DOT 2021).

Table 1. Pavement Condition Indices Southern Region (Adapted from Papagiannakis (2009); Bektas (2014)). (Continued).

State	Distresses Collected	Pavement Condition Index
North Carolina	Structural and non-structural cracking, rutting, ride quality, patching and bleeding.	Pavement Condition Rating (scale of 0-100) is used. Deduct values are calculated based on the primary distresses listed.
Oklahoma	Structural and non-structural cracking, rutting, ride quality, faulting and slab cracking.	Pavement Quality Index (PQI) is calculated using weight factors and individual indices depending on pavement type, such as Ride Index, Rutting Index, and Faulting Index, among others.
South Carolina	Ride quality index, rutting and distress.	PQI is calculated based on two individual indices (0 to 5 scale); Pavement Distress Index (PDI) (0 to 5 scale) and Pavement Serviceability Index (PSI) based on an IRI correlation.
Tennessee	Ride quality index, rutting and distress.	PQI calculated also from PDI and PSI but using a different relation between the two indices.
Texas	Multiple distresses according to pavement type listed by Stampley et al. (1995).	Condition Score (CS), scaled between 0 and 100. Index is explained in subsection 2.5.2.

2.5.5 CALCULATION OF PAVEMENT CONDITION RATING (PCR) USED BY MDOT

As already mentioned, PCRs are condition indices that combine multiple distress types, extensions and severities into a single score. MDOT considers 12 pavement distresses for the four pavement types, as **Error! Reference source not found.** shows. Nevertheless, multiple distresses h ave been removed from the analysis due to their low frequency such as pumping, map cracking, blow ups, edge cracking, edge cracking, raveling, reflective cracking, and block cracking, among others (Pathway Services Inc 2016). This evaluation is achieved using video images and digitalized measurement of distress areas, lengths, and widths, as explained in further sections. All distresses are analyzed automatically, with the few exceptions of corner breaks and punchouts.

Table 2. Predominant Distresses on PCR calculation (Pathway Services 2016).

Pavement	Distress Type	Severity Levels	Type of Measurement
All	Longitudinal Cracking	Low, Medium, High	Length (ft.)
All	Transverse Cracking	Low, Medium, High	Length (ft.)
All	Patching	Low, Medium, High	Area (sq. ft.)
JCP	Durability Cracking	Low, Medium, High	Area (sq. ft.)
JCP	Spalling-Longitudinal	Low, Medium, High	Length (ft.)
JCP	Spalling-Transverse	Low, Medium, High	Length (ft.)
JCP	Faulting of transverse joints	Low, Medium, High	Average Depth (inch)
JCP	Corner Breaks	Low, Medium, High	Quantity (count) & Area (sq. ft.)
CRCP	Punchouts	Low, Medium, High	Quantity (count) & Area (sq. ft.)
FLEX	Fatigue Cracking	Low, Medium, High	Area (sq. ft.)
FLEX/COMP	Potholes	Low, Medium. High	Quantity (count) & Area (sq. ft.)

Densities are calculated from the distresses in the analysis sections. The total section area is estimated using the section length times the lane width (not to exceed 12 ft). For area distresses like alligator cracking, the density is determined with the total area of cracking divided by the total area of the section. In the case of linear distresses, like longitudinal cracking, it is necessary to convert the length or width to an affected area. Consequently, MDOT has assumed a width of 1in for all linear-distress severities. Density is also calculated with the total distress area divided by the total area of the section. The same process is done for countable distresses as corner breaks or potholes, where an area is quantified, and used to determine severity levels. On the other hand, for length/width distresses as spalling, density is calculated by dividing the calculated distress area by the total section length.

In addition to the described distresses, MDOT collects rutting depth and roughness (MRI) data that is also used for the PCR calculation process. With the densities defined, MDOT has used deduct points (DP) for each distress type and severity level. Deduct points are multiplied by each distress density, added together, and introduced on a regression model (depending on pavement type) for obtaining the PCR. Table 3 presents an example of some deduct values for flexible pavements. Equation 5 through Equation 8 describe the regression models for each pavement type, where "TPD" represents the sum all deduct points for every distress type and severity level. TPD is calculated by the sum of the product of each experienced distress density and its respective utility value. Figure 11 illustrates the PCR calculation process.

Table 3. Deduct points example for flexible pavement

Parameter	Deduct Point	Severity
Rutting (mm)	0.05	1.5 <= x < 3.0mm
	0.09	3.0 <= x < 6.25mm
	0.14	x>= 6.25mm
Fatigue Cracking (%)	0.45	Low
	0.64	Medium
	0.94	High
Longitudinal Cracking (%)	3.00	Low
	6.00	Moderate
	9.00	High
MRI (mm/m)	10.50	-
Potholes (area)	20.00	Low, Moderate, High

Flexible Pavement (FLEX):

$$PCR = 0.94\,x\,(\,(0.0008\,x\,(TDP)^2) - 0.7022\,x\,TDP) + 102.48) \quad \text{Equation 5}$$

Jointed Concrete Pavement (JCP):

$$PCR = 0.94\,x\,(\,(-4x10^{-5}x\,(TDP)^2) - (0.4777\,x\,TDP) + 90.812) \quad \text{Equation 6}$$

Composite Pavement (COMP):

$$PCR = 0.94\,x\,((0.0007\,x\,(TDP)^2) - (0.536\,x\,TDP) + 97.578) \quad \text{Equation 7}$$

Continuously Reinforced Concrete Pavement (CRCP):

$$PCR = 0.94\,x\,((-0.001\,x\,(TDP)^2) - (0.799\,x\,TDP) + 98.754) \quad \text{Equation 8}$$

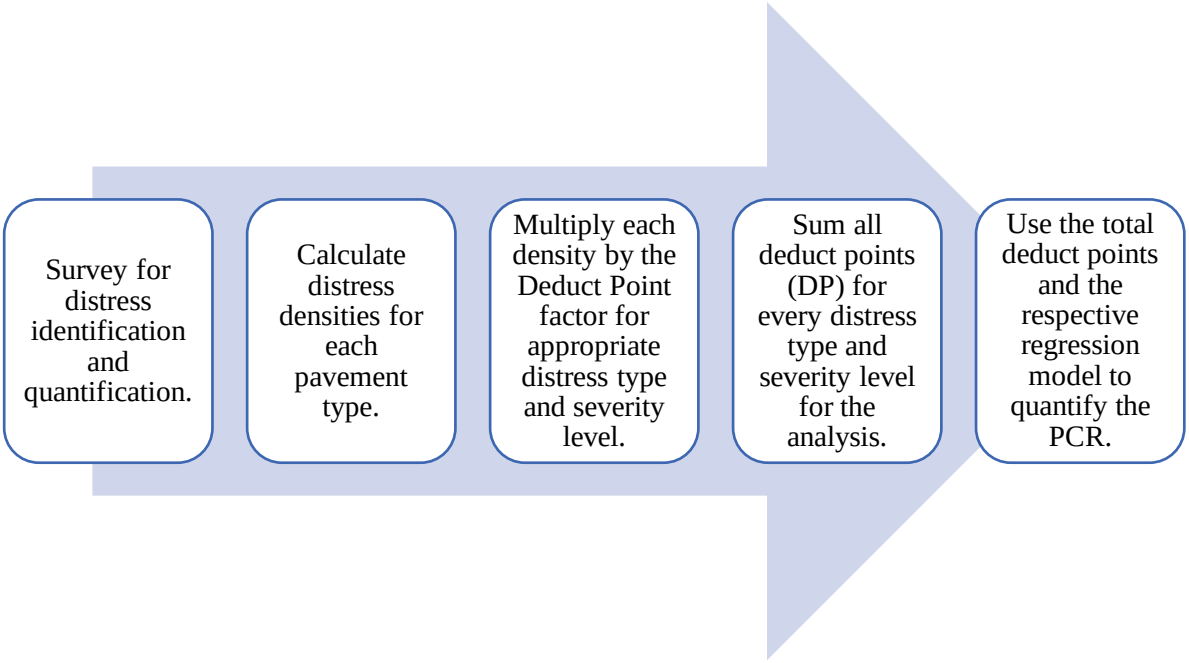

Figure 11. MDOT's PCR quantification process.

2.5.6 DECISION TREES FOR MAINTENANCE AND REHABILITATION ACTIVITIES USED BY MDOT

Even though MDOT uses PCRs for high-level reporting to upper management, M & R activities are planned according to decision trees. Decision trees incorporate three principal distresses selected by MDOT (rutting, faulting, and ride quality, expressed by MRI). Five different categories are generated according to the mentioned indicators. Table 4 presents the defined thresholds for each category and the typical PCR ranges that a pavement in each category may have. Nevertheless, MDOT has classified PCRs into three main categories (poor, fair, and good condition) for presenting to road users and stakeholders, as shown in Figure 12. In addition, MDOT has established a goal of maintaining interstate pavements in good condition and all other State Maintained highways at a minimum fair condition (MDOT 2022).

Table 4. Thresholds for MDOT decision trees.

Very Good – VG	New or almost new pavement, will not require improvement for some time
MRI (in/mile)	<59.6
Rutting (in)	< 0.06 or 1/16
Faulting (in)	< 0.13 or 1/8
PCR	>= 89
Good -- G	In satisfactory condition, will not require improvement in the near future
MRI (m/km)	59.6 <= x < 93.8
Rutting (in)	0.06 or 1/16 <= x < 0.13 or 1/8
Faulting (in)	0.13 or 1/8 <=x < 0.25 or 1/4
PCR	82 < = x < 89
Fair – F	Will likely need improvement in the near future, but depends on traffic use
MRI (in/mile)	93.8 <= x < 114
Rutting (in)	0.13 or 1/8 <= x < 0.25 or 1/4
Faulting (in)	x>0.25
PCR	72 <= x < 82
Poor – P	Needs improvement in the near future to preserve usability
MRI (in/mile)	114 <= x < 164.8
Rutting (in)	0.25 or 1/4 <= x < 0.50 or 1/2
Faulting (in)	0.50 or 1/2 <= x < 0.75 or 3/4
PCR	63 <= x < 72
Very Poor – VP	Needs improvement to restore serviceability
MRI (in/mile)	>164.8
Rutting (in)	>= 0.50 or 1/2
Faulting (in)	>= 0.75 or 3/4
PCR	< 63

Figure 12. PCR classification used by MDOT (MDOT 2022)

2.5. SUMMARY

This chapter conceptualized the importance and main functions of a pavement management system. Additionally, pavement distresses commonly experienced on MDOT's pavement structures were described according to their severity level and pavement type. Moreover, this literature review provided information about the pavement longitudinal profile assessment, where IRI has been a predominant index for describing pavement roughness.

In relation to the pavement rating systems, three main scoring methods have been implemented by agencies (direct panel rating, utility functions, deduct values, and weighting factors). Nevertheless, the distresses accounted, severity levels, and condition indices used in these scoring methods vary between agencies. Therefore, the definition of procedures adjusted to experienced conditions is a fundamental step for a realistic pavement assessment and scoring

CHAPTER 3: METHODOLOGY

This section comprises the procedures followed to achieve the defined objectives. As already described, the data collection process is an inherent function of every PMS. During this activity, agencies gather pavement distress, frequency and severity according to previously defined guidelines. Moreover, data quality is assessed by the same consultants who perform the collection process. Finally, data is processed to determine the individual and overall ratings of the multiple pavement sections that made up the network. MDOT repeats this process every two years to assess the pavement network condition, inform authorities, and determine required M&R activities. The following sections describe the multiple steps included in the condition assessment procedure.

3.1 DATA COLLECTION AND DISTRESS IDENTIFICATION PROCESS

MDOT focuses on collecting four primary types of data (inventory, construction, pavement condition and, "other" data). Inventory data comprises the geometric elements and route information from the road network. Construction data includes the information on new pavements constructed, as well as rehabilitation projects. Pavement condition data comprises the previously listed pavement distresses and ride quality. "Other data" involves information about the structural assessment of existing pavements (falling weight deflectometer data) and skid/friction data. Even though MDOT's PMS encompasses several data types, this project focuses on pavement condition or distress data.

MDOT hires external vendors or contractors to perform the distress surveys. Vendors conduct these distress surveys using a van equipped with profilers and photologging devices. According to Duncan et al. (2017), longitudinal and transverse profiles are collected utilizing a South Dakota profiler with multiple laser sensors that capture roughness, rutting, and faulting measurements. Five video cameras are mounted on the van to capture images of the pavement surface and identify other distresses. These images are digitized into frames for an automated distress recognition process. Additionally, the survey van has a GPS receiver that assigns coordinates to the collected data.

During the distress identification process, pavement lane locations are broken down as left edge (LE), left wheel path (LWP), center (CEN), right wheel path (RWP), and right edge (RE), as shown in Figure 13. This location division allows to identify the distresses that are manifested in certain spots according to their nature (e.g., fatigue cracking is only assessed in LWP and RWP, meanwhile longitudinal cracking is assessed in RE, LE and CEN, excluding both wheelpaths). Additionally, only those distresses that fall inside the white marks will be included in the distress analysis procedure (Pathway Services Inc 2016). For simplicity in the analysis, pavement width has been considered as the horizontal measurement across the lane and pavement length has been referred to as the vertical measurement on the roadway.

Sealed cracks are properly identified and excluded from the cracking counting process. Bridge pavement data is also excluded from the analysis. For instance, bridges are defined by the construction joints found at the beginning and end of each bridge's structure.

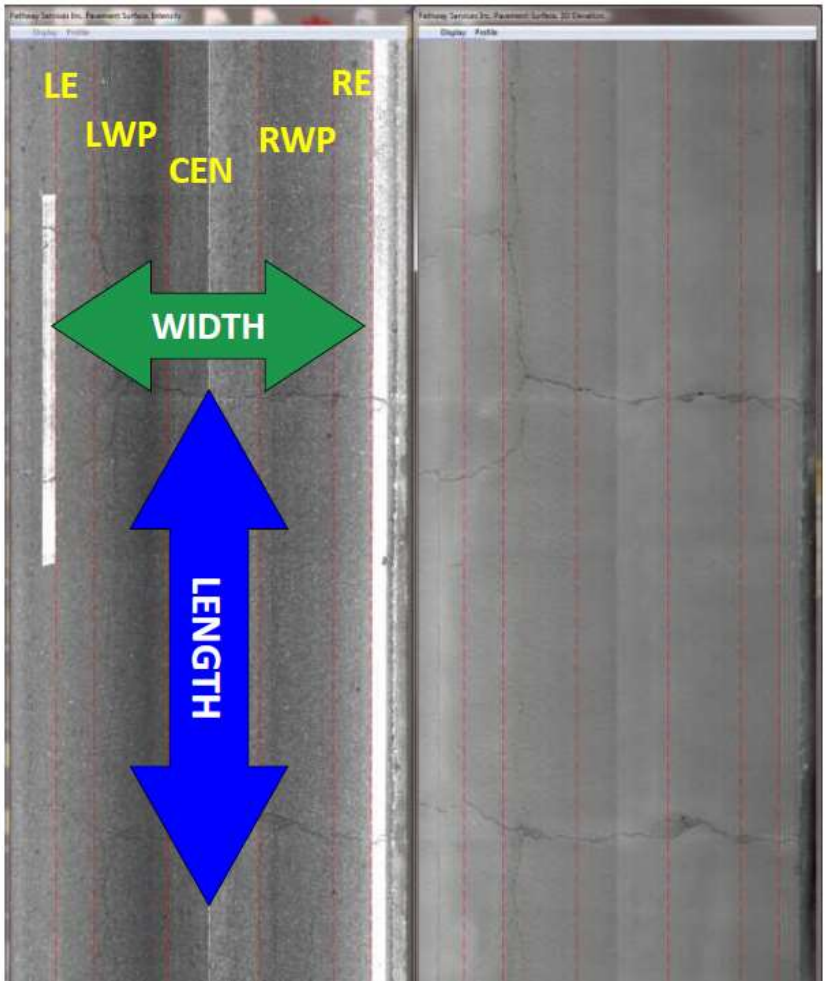

Figure 13. Lane Breakdown for Distress Identification. (Pathway Services Inc 2016).

After pavement condition data is collected, quality control and quality acceptance procedures are performed according to MDOT's quality management plan (Duncan et al. 2017). For this specific project, all the data provided by MDOT has already passed through this filtering. Nevertheless, the cumulative distribution functions for each of the distresses were evaluated in order to identify their specific distributions, and possible atypical measurements on the database.

3.2 DATABASE DESCRIPTION

The data provided by MDOT included multiple files with information about the biannually surveyed pavement sections. It comprised observations from 1995 to 2020. Data were extracted into a single file for each pavement type (FLEX, JCP, COMP and CRCP). As requested by MDOT, a previous stage of this project evaluated the possibility of reducing the predominant distresses list presented in Table 2. In that first stage, normalized count analyses and cumulative density functions were applied in order to understand the frequency of each distress type (Chowdari 2019). It was determined that several distresses can be excluded from the scoring process without significantly affecting the resulting PCR. To cite an instance, only 5% of the flexible sections in the network have 1 to 2 potholes per mile of any severity level and only 5% of the sections have 2 to 3 patches per mile. Remaining distresses like alligator, longitudinal, and transverse cracking were frequent in flexible pavements (Chowdari 2019). Figure 14 illustrates the relationship between the PCR calculated with all distresses and the PCR calculated without accounting for potholes and patching. It can be observed that the majority of data points fall along the identity line.

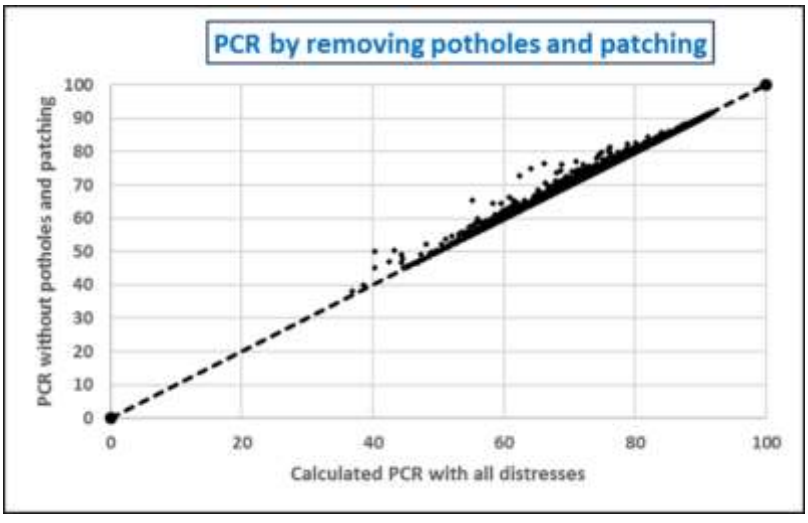

Figure 14. Comparison of PCR with all distresses and PCR without potholes and patching (Chowdari 2019).

Data from the 2020 survey was not available at the time that the reduction of the predominant distresses was being researched; consequently, a similar process was performed on this data. As Figure 15 illustrates, there was no significant impact when excluding the less frequent distresses for the different pavement types. Therefore, the existing database was reduced to the following distresses, according to each pavement type:

- FLEX: potholes and patching were excluded from the predominant distresses list. Predominant distresses included longitudinal and transverse cracking (non-structural cracking), and alligator cracking (structural cracking). Additionally, MRI and rutting measurements were maintained for the PCR calculation process.
- JCP: transverse and longitudinal spalling, D-cracking, patching and corner breaks were excluded from predominant distresses list. Distresses and performance indicators accounted on PCR calculation include longitudinal and transverse cracking, MRI and faulting.
- CRCP: punchouts were eliminated from the predominant distresses list. PCR calculation considered longitudinal and transverse cracking and MRI measurements.
- COMP: potholes and patching were excluded from the predominant distresses list. This list was reduced to longitudinal and transverse cracking, rutting and MRI measurements for this specific pavement type.

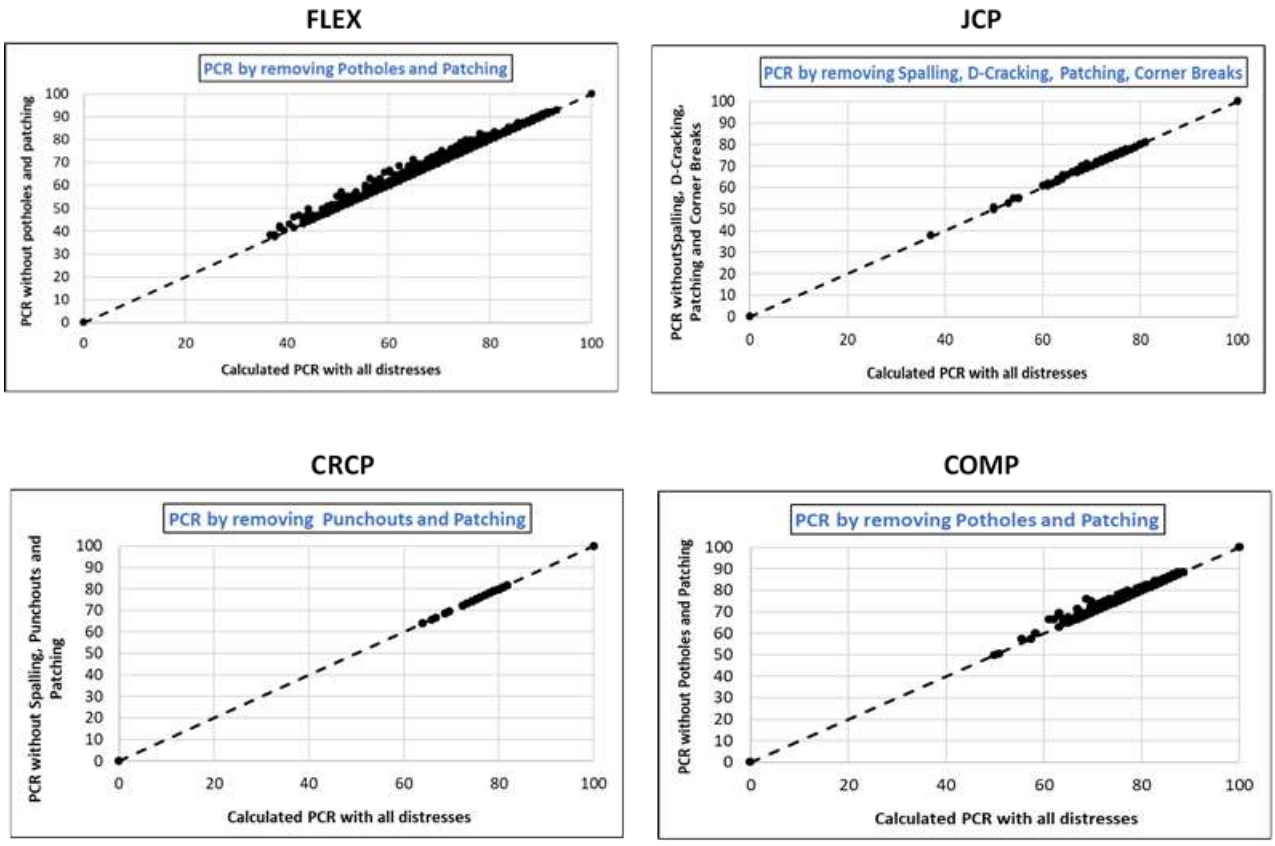

Figure 15. Comparison of PCR with all distresses and PCR without less frequent distresses.

A detailed description for each pavement type which includes the predominant distress distributions and its respective Pearson correlation coefficient when compared to other distress indicators is given in Appendix 1.

3.3 DISTRESS DENSITIES

The definition of the different distress densities is a fundamental step in any pavement scoring procedure. Densities allow quantifying the magnitude of a specific pavement distress and comparing different sections from an individual distress perspective. Therefore, the following elements describe the procedures followed to quantify these densities.

- Structural Cracking: alligator cracking was quantified by implementing a cracking area concept, in which the measured cracking area was related to a portion of the section area and represented as a percentage. As already explained, structural cracking area measurements were just collected from both wheelpaths; therefore, the section area was delimited by the section length and a wheelpath width of 3ft (value used by MDOT). Figure 16 illustrates part of the process, and Equation *9* shows the calculation procedure.

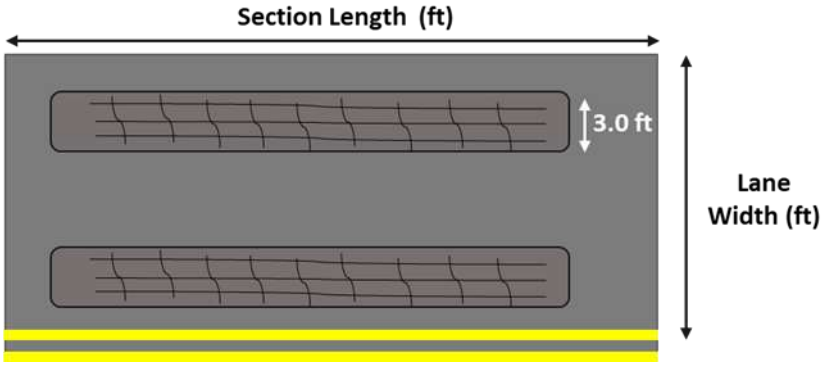

Figure 16. Structural cracking density determination.

$$\text{Structural Cracking (\%)} = \frac{\text{Alligator Cracking Area Area}(\text{ft}^2)}{\text{Section Length (ft) x 2 x (3.0 ft)}} x\ 100 \qquad \text{Equation 9}$$

- Non-Structural Cracking: transverse and longitudinal cracking extent is given by the sum of the lengths in feet, as defined by the Standard Practice for Quantifying Cracks in Asphalt Pavement Surfaces from Collected Pavement Images Utilizing Automated Methods AASHTO PP 67-16 (2017). Furthermore, the same document highlights that the agency is free to utilize the reported data as best fits its pavement

management needs. However, it is warned that dividing the scalar extent and severity values into level categories or bins can result in erratic results.

Even though crack severity was defined by differences in crack width and multiple pixel configurations, crack width was not reported in the database. Therefore, to prevent any inaccurate assumptions, a linear density relation was followed, as illustrated by Figure 17 and presented in Equation 10.

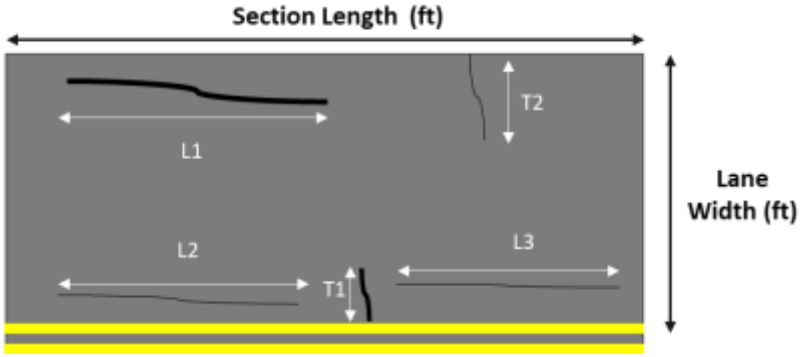

Figure 17. Density definition for linear cracking.

$$\text{Non} - \text{Structural Cracking (\%)} = \frac{\text{Longitudinal} + \text{Transverse (ft)}}{\text{Section Length (ft)}} x\ 100 \qquad \text{Equation 10}$$

It is important to highlight that all the analyzed sections included their respective length. However, this was not the case for the width, which was missing for some sections. Therefore, an external file with the sections' widths was requested and provided by MDOT. Specifically, it included almost 6000 sections with their respective width and identifier (ID). This last parameter was utilized for linking the dimension to the existing database.

- Faulting, Rutting, and MRI: several continuous variables such as faulting, rutting and MRI were registered and interpreted using their respective measurement units (e.g., faulting was expressed and interpreted in inches).

3.4 INDIVIDUAL DISTRESS-SEVERITY RATING MODELS

Before calculating the PCRs, MDOT requested to have individual distress-severity rating models for each of the distresses considered. Therefore, the definition of reasonable scores for each distress magnitude was an inherent task developed in conjunction with MDOT. Specifically, MDOT engineers provided a "proposed score" for several rutting, faulting and MRI magnitudes with a maximum score of 100 and capped to a certain value. Figure 18 shows an example of the proposed scores plotted against the MRI values.

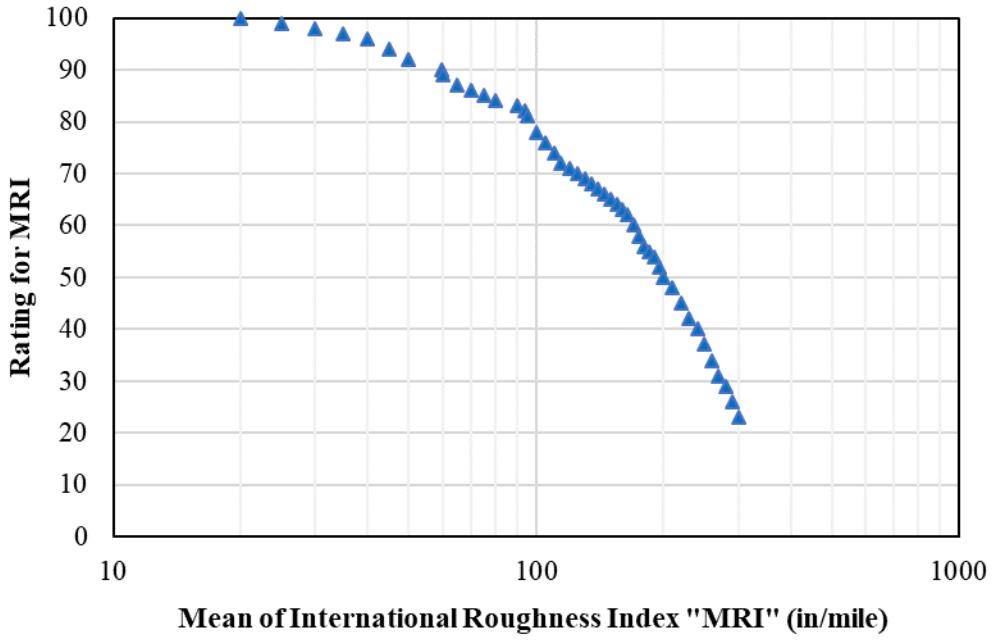

Figure 18. MDOT proposed scores for MRI values.

A model was fitted using the proposed scores. Specifically, a log-based sigmoidal curve was selected for two main reasons. First, as explained in the previous chapter, sigmoidal curves have been well-known for accurately describing pavement performance. Second, according to Onofri (2019), log-based sigmoidal curves are functions where the independent variable is constrained to be positive (similarly to PCR). Consequently, using a function that is also defined for negative numbers (e.g., polynomial functions) may seem unrealistic in PCR terms. Equation 11 describes the selected model and Figure 19. Log-logistic sigmoidal curve (Adapted from: Onofri (2019))illustrates its typical shape.

$$\mathrm{Y} = c + \frac{\mathrm{d} - \mathrm{c}}{1 + \left(\frac{X}{e}\right)^{b}} \qquad \text{Equation 11}$$

Where:

b: slope factor.

c: score at zero distress concentration.

d: score at “unlimited” distress concentration.

e: inflection point.

X: distress density.

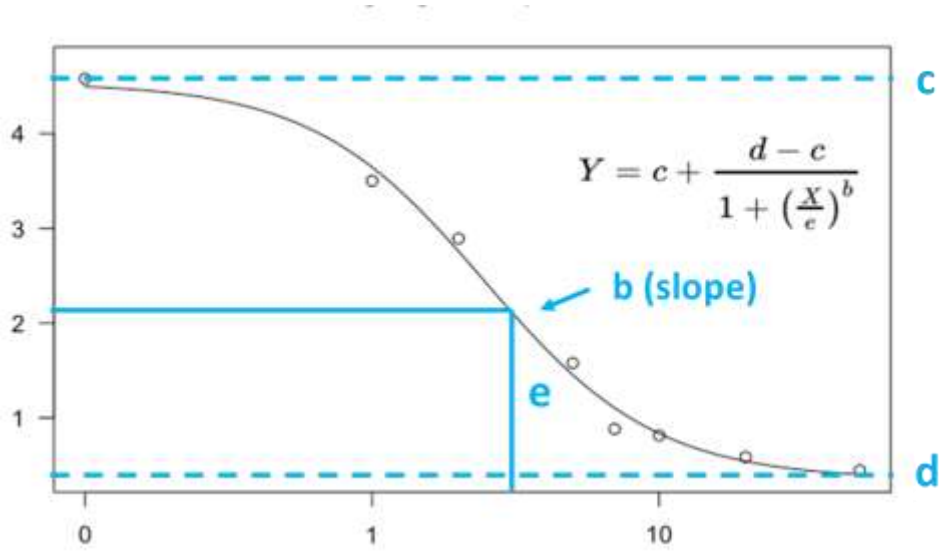

Figure 19. Log-logistic sigmoidal curve (Adapted from: Onofri (2019)).

In terms of cracking, there was no proposed scoring method from MDOT. Therefore, it was suggested and agreed to create the scoring curves following a similar trend to the ones developed in the ASTM D6433 standard. In addition, the described log-logistic model was selected to maintain consistency. Models were developed and revised for each severity level and cracking type.

3.5 PCR CALCULATION PROCESS (WEIGHT FACTORS)

With the individual scores or indices for each pavement distress already defined, the next step was to combine all those ratings into a single score (PCR). However, combining those individual indices was not the only task, since MDOT wanted to prevent any abrupt changes in the PCR values when compared to previous years. These possible changes would incorrectly be perceived as road network improvement or deterioration if, for similar pavement conditions, the new calculated PCRs were significantly higher or lower than the ones calculated using the previous method. Therefore, this task involved two main functions, assigning a weight for each individual score and trying to match the calculated PCR to the historical data as much as possible.

Consequently, the evaluation of coefficients or weight factors capable of performing both functions was considered. Figure 20 illustrates part of the PCR calculation sequence for the flexible pavement.

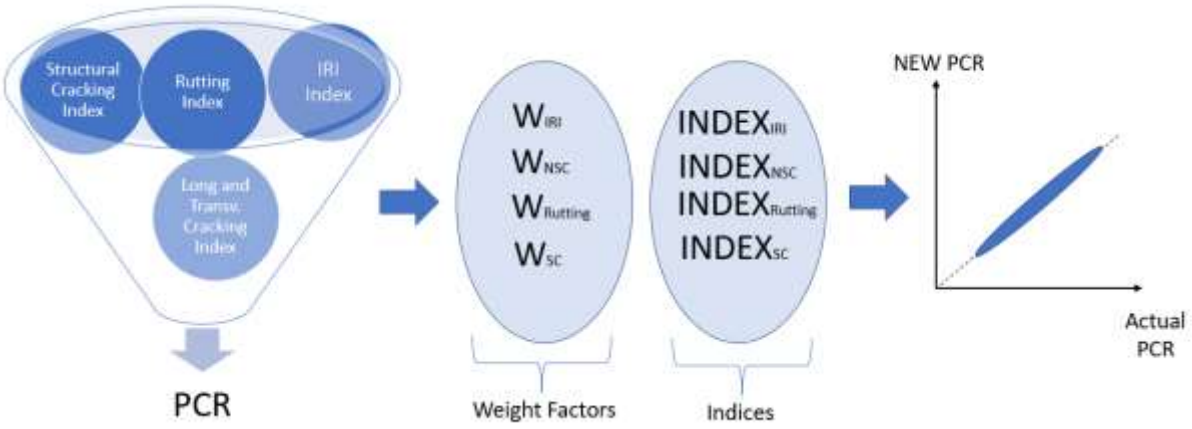

Figure 20. PCR calculation sequence, FLEX example.

In order to achieve these two main elements, a least squares procedure was followed. Shtayat et al. (2022) have indicated that a least of squares regression is a simple technique that requires a minimum number of parameters, and it is suitable in pavement classification and recognition works. According to the National Institute of Standards and Technology (2012), least of squares is a commonly used technique in linear regression analysis, in which individual coefficients are multiplied by their respective independent variable, then results are added together. These coefficients are defined by minimizing the sum of the squares of the residuals (difference between an historical observation and a value predicted from a fitted model). In this specific case, historical measurements were the PCR values calculated with the old method, meanwhile, predicted values were the PCRs calculated by the method developed in this document (individual scores). Moreover, the obtained coefficients are referred to as weight factors in this document. Equation 12 shows the general PCR calculation procedure for all pavement types.

$$\text{PCR} = \sum_{i=1}^{n} [(\text{Distress Index}_n) \text{ x } (\text{Weight Factor}_n)] \qquad \text{Equation 12}$$

A "New PCR" was calculated using the respective condition data. Then, the squared difference between the new PCR and the historical PCR (calculated with the old method) was performed. This process was repeated for all the observations, and added together, as presented by Equation 13. The weight factors selected corresponded to the minimum sum of squared residuals. Additionally, Figure 21 illustrates the general process for calculating PCRs for each pavement type.

$$\text{Sum of Squared Residuals} = \sum_{i=1}^{n} [(\text{PCR by DOT}_n) - (\text{New PCR}_n)]^2 \qquad \text{Equation 13}$$

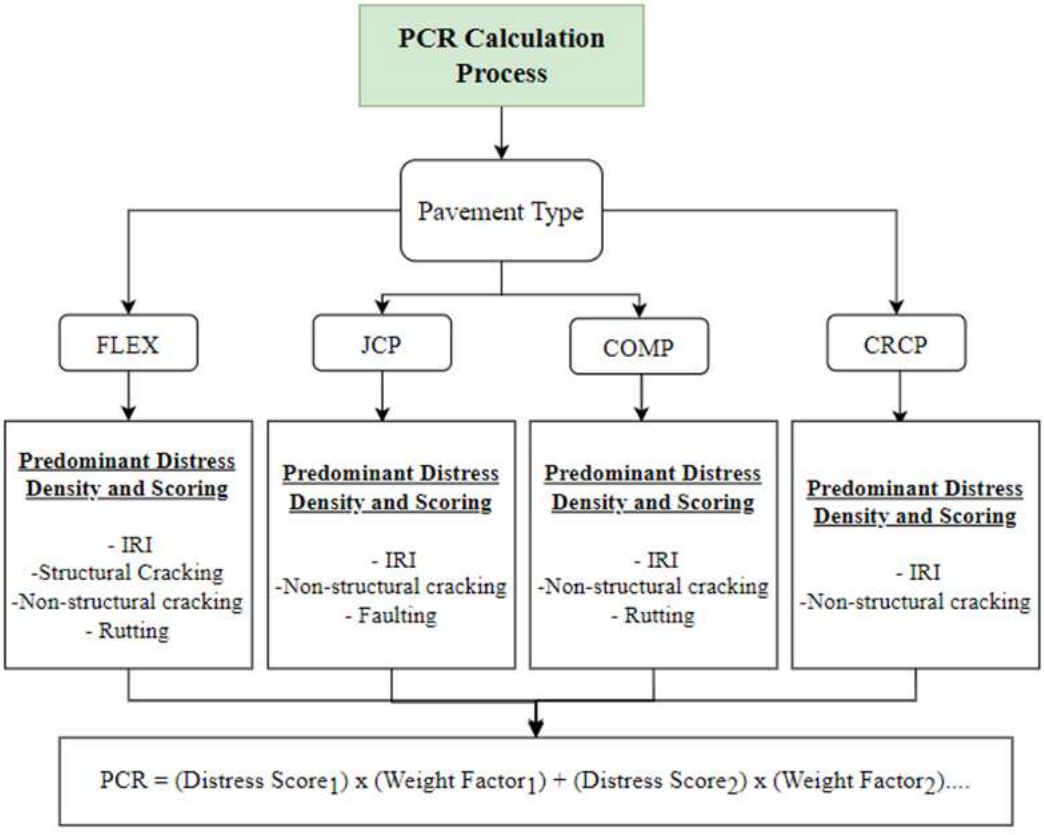

Figure 21. PCR general calculation flowchart.

3.5.1 DATA SPLITTING METHODS

As in every model development, the dataset partitioning for model fitting and validation is a fundamental activity to prevent any bias in the model. For this case two different data splitting methods were evaluated. Initially, it was proposed to fit the models using the data from 1995 to 2018 and validate them using the 2020 data (time-based splitting). This suggested procedure was based on the preliminary idea that using the most recent data (2020) to validate the model could help to understand the model's performance better. However, this could lead to an exclusion of an important and recent portion of the data from the training procedure. Therefore, a random splitting method was also considered in the process.

To test these described differences, a small experiment was conducted. Specifically, using the FLEX pavement data, models were trained and validated by applying both data splitting methods (time-based and randomly splitting). Actual observations (historical PCRs) were compared against predicted PCRs to assess the models' error. Even though there have been multiple methodologies for randomly splitting data (e.g., stratified splitting, different splitting ratios), a complete analysis of all of them was beyond the scope of this project. A commonly used ratio of 80:20 was selected (80% of the data is for training and 20% for testing). According to Roshan (2022), despite there being no be clear guidelines on what ratio is optimal for a given dataset, the 80:20 split draws its justification from the well-known Pareto principle. Figure 22 illustrates the two data splitting methods evaluated.

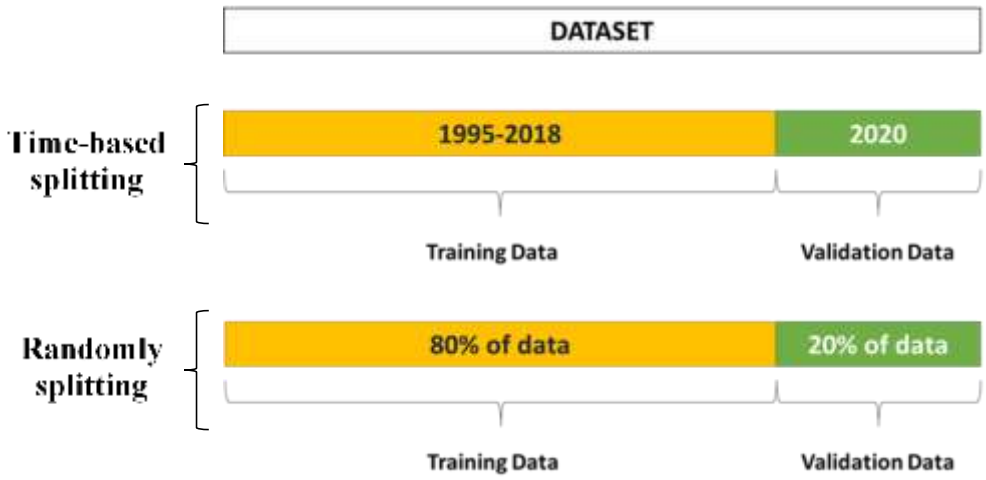

Figure 22. Data splitting methods.

For the randomly splitting process iterations were performed to evaluate the model performance through different statistical indicators such as root squared mean error (RSME), mean absolute error (MAE), and the coefficient of determination (R^2) (explained in further sections). Specifically, 52 091 observations were randomly divided into an 80:20 ratio; models were trained, validated, and PCR predictions were compared against observations for both processes (validation and training). Table 5 shows the results for each of the iterations.

Table 5. Model evaluation using randomly splitting method (training and validation).

Iteration	Training			Validation		
	RSME	MAE	R2	RSME	MAE	R2
1	6.312	4.379	0.699	6.222	4.295	0.705
2	6.260	4.343	0.702	6.426	4.439	0.695
3	6.279	4.358	0.700	6.353	4.379	0.702
4	6.278	4.353	0.704	6.356	4.402	0.684
5	6.298	4.370	0.700	6.277	4.334	0.702
6	6.306	4.376	0.700	6.244	4.310	0.701
7	6.310	4.374	0.700	6.227	4.316	0.700
8	6.271	4.351	0.701	6.385	4.410	0.696
Average	6.289	4.363	0.701	6.311	4.361	0.698
Standard Deviation	0.020	0.013	0.002	0.078	0.054	0.007

As shown in Table 5 and summarized in Table 6, the average difference between the validation error and training error was close to each other, which can be related to a possible irreducible error and a desirable behavior on model fitting terms. On the other hand, Table 7 presents the results for the time-based splitting method (4499 observations for validation), in which a greater error for both training and validation was experienced, a possible sign that this data splitting method is leading to underfitting problems. Based on these results, the randomly splitting method was selected for the development of the PCR models.

Table 6. Training and validation average errors for randomly splitting method.

Splitting Method	Dataset	RSME	MAE	R2
Random Splitting	Training	6.289	4.363	0.701
	Validation	6.311	4.361	0.698
Difference (%)	-	0.347	0.053	0.382

Table 7. Training and validation error for time-based splitting method

Splitting Method	Dataset	RSME	MAE	R2
Time Series	Training	6.459	4.501	0.683
	Validation	6.834	4.844	0.746
Difference (%)	-	5.806	7.621	9.224

3.6 STATISTICAL INDICATORS (MODEL EVALUATION)

This section describes the indicators utilized to assess the model fitting accuracy and agreement with the historical data. Measuring the agreement of a new rating procedure against a defined standard or a previous rating method is a fundamental activity to determine if the evaluated systems can be replaced by each other. Multiple indicators have been implemented to assess this activity, nevertheless, their interpretation and functionality vary among them. Four different statistical indicators were used in this project and are explained in the following subsections.

Additionally, a confuse matrix technique was utilized for the validation dataset to evaluate the defined models in different PCR ranges.

3.6.1 COEFFICIENT OF DETERMINATION (R^2)

The coefficient of determination has been a widely implemented indicator to express the model fitting. Commonly, R^2 is interpreted as the percentage of variation in the dependent variable explained by variation in the independent variables (Filho et al. 2011). This value ranges from 0 to 1, where 1 represents a perfect fit, while 0 implies that the model fails to represent the data. Even though R^2 implies an estimated relationship between the dependent and independent variables, it does not express if the chosen model is adequate, nor if the predictions are biased (Filho et al. 2011). Therefore, evaluating multiple indicators can result in a clearer perspective. Equation 14 shows how R^2 was calculated.

$$R^2 = 1 - \frac{\sum_{i=1}^{n}(\hat{y}_i - y_i)^2}{\sum_{i=1}^{n}(y_i - \bar{y}_i)^2} \qquad \text{Equation 14}$$

Where:

$\hat{y}_i$: predicted value, PCR predicted from the model.

$\bar{y}_i$: mean of actual values, mean of historical PCRs.

y_i: actual value, historical PCR.

3.6.2 ROOT MEAN SQUARE ERROR (RSME) AND MEAN ABSOLUTE ERROR (MAE)

RSME and MAE are commonly used indicators to determine model accuracy for continuous variables. According to Chai and Draxler (2014), RSME is a quadratic scoring indicator that quantifies the average magnitude of the error between two databases (predicted vs given) as Equation 15 shows. MAE quantifies the absolute average magnitude of the errors between the predicted and given variables, as shown in Equation *16*.

$$\mathrm{RSME} = \sqrt{\frac{1}{n}\sum_{i=1}^{n}(y_i - \hat{y}_i)^2} \qquad \text{Equation 15}$$

$$\mathrm{MAE} = \frac{1}{n}\sum_{i=1}^{n}|y_i - \hat{y}_i| \qquad \text{Equation 16}$$

Where:

$\hat{y}_i$: predicted value, PCR predicted from the model.

y_i: actual value, historical PCR.

n: number of observations.

Both RMSE and MAE express the average model prediction error in units of the variable of interest, in this case, PCR units. Therefore, lower RSME/MAE values correlate with higher model accuracy. Additionally, since the errors are squared before they are averaged, the RMSE can be more susceptible to outliers (Chai and Draxler 2014). Therefore, the same authors recommend that analysis of both indicators is often required to assess model performance from a broader scope.

3.6.3 CONCORDANCE CORRELATION COEFFICIENT (CCC)

The CCC is an index that states the correlation between two observations that fall on the 45-degree line through the origin (identity line) (Lin 1989). This index ranges between -1 and 1, where a value of 1 signifies a perfect positive correlation (paired observations fall precisely on the identity line). Meanwhile, values close to -1 reveal strong discordance, and values near zero indicate no concordance at all. This would suggest that this index follows the same principle as the Pearson correlation coefficient; however, they are different as Figure 23 illustrates.

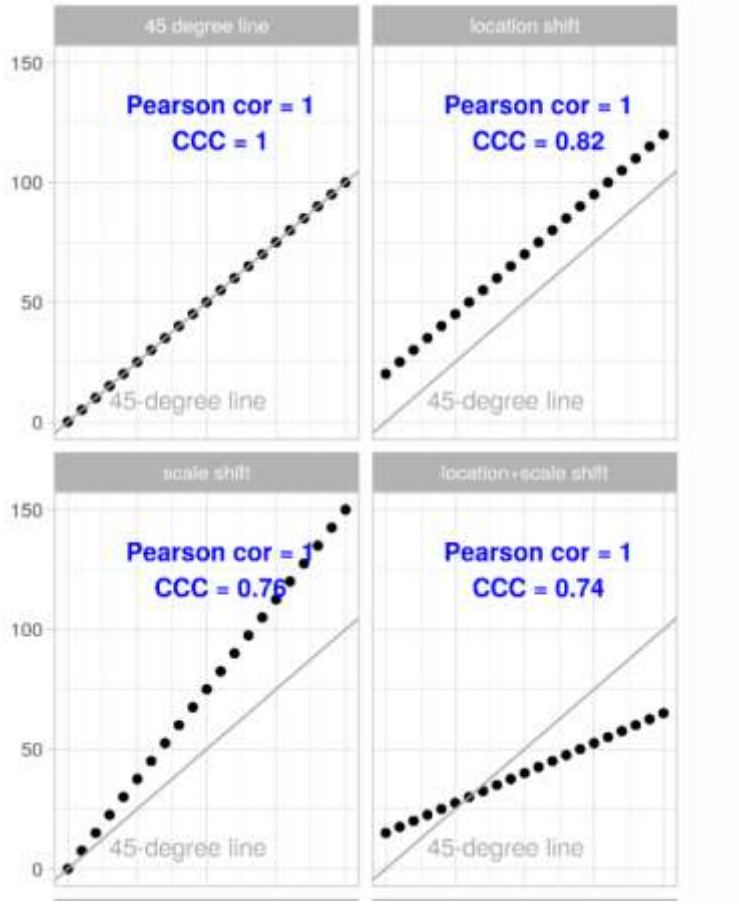

Figure 23. CCC vs Pearson Correlation Coefficient (Gossman 2020).

As shown in Figure 23, the Pearson correlation coefficient is used to quantify the extent to which measurement pairs can be described by a linear equation, with any intercept and slope. On the other hand, CCC is a better metric for assessing measurement reproducibility between different rating methods since it indicates how close the measurement pairs fall to the 45-degree line (Gossman 2020). CCC is calculated according to Equation 17.

$$\mathrm{CCC} = \frac{2 \text{ x } \sigma_1 \text{ x } \sigma_2}{(\mu_1 - \mu_2)^2 + \sigma_1^2 + \sigma_2^2} \qquad \text{Equation 17}$$

Where:

μ_1: average predicted value, average predicted PCR.

μ_2: average historical value, average historical PCR.

σ_1: variance of predicted values predicted PCR.

σ_2: variance of historical values, historical PCR.

Even though there has not been a defined criterion for interpreting CCC values, some authors, have interpreted Lin's CCC the same way as the Pearson correlation coefficients, in which CCC values below 0.20 indicate a poor agreement, while values above 0.80 indicate an excellent agreement (Altman 1991). McBride (2005), proposed more strict criteria for laboratory applications, in which CCC values between 0.95 and 0.99 indicate a substantial agreement, values between 0.90 and 0.95 indicate a moderate agreement, and values below 0.90 reveal a poor agreement.

3.6.4 CONFUSION MATRIX

A confusion matrix is a machine learning tool used for summarizing the performance of a classification algorithm or model. Specifically, it encapsulates the number of correct and incorrect predictions for previously defined classes or categories (Piryonesi and El-Diraby 2018). Confusion matrices are commonly applied for model validation, in which validation data is input into the defined model and assessed through this analysis technique. Figure 24 illustrates an example of a confusion matrix for a pavement condition index (PCI) prediction model, in which the number of correct predictions for each class, and the number of incorrect predictions (organized by the class that was predicted) are counted.

Table 3. Confusion matrix of a C4.5 trained by 942 examples.

Pred./Act. PCI	Actual Good	Actual Satisfactory	Actual Fair	Actual Poor	Actual Very Poor	Actual Serious	Actual Failed	Class Precision
Predicted good	180	38	18	1	1	0	0	75.6%
Predicted satisfactory	16	98	26	7	2	1	0	65.3%
Predicted fair	7	23	161	14	10	6	0	72.9%
Predicted poor	2	3	22	91	19	6	0	63.6%
Predicted very poor	0	2	10	14	92	11	3	69.9%
Predicted serious	0	1	4	2	11	30	4	57.7%
Failed	0	0	0	0	0	5	1	16.6%
Class recall	87.8%	59.4%	66.8%	70.5%	67.6%	50.8%	20.0%	—

Figure 24. Confusion matrix for PCI model (Piryonesi and El-Diraby 2018).

As shown in Figure 24, there are three main indicators in the confusion matrix (class recall, class precision and accuracy). The class recall is the ratio of the correctly predicted observations for a specific class and its total number of observations, as Equation *18* reveals. Class precision is the measure of how close the predicted values are to each other; it is calculated according to Equation 19. Finally, accuracy represents how close the correctly predicted values are to the actual values, and it is calculated according to Equation 20.

$$\text{Class Recall} = \frac{\text{Correctly predicted values from a specific class}}{\text{Total actual values from a specific class}} \text{ x } 100 \qquad \text{Equation 18}$$

$$\text{Class Precision} = \frac{\text{Correctly predicted values from a specific class}}{\text{Total predicted values from a specific class}} \text{ x } 100 \qquad \text{Equation 19}$$

$$\text{Accuracy} = \frac{\text{Correctly predicted values}}{\text{Total number of observations}} \text{ x } 100 \qquad \text{Equation 20}$$

3.7 SUMMARY

This chapter described the procedures followed for developing the MDOT PCR rating system. Initially, a brief description of how pavement performance data is collected and presented by consultants hired by MDOT was given. Then, the predominant distresses included in the PCR calculation process were assessed. Densities were defined according to each distress type. Moreover, the steps followed for developing an individual rating for each distress type and severity, based on MDOT recommendations and sigmoidal functions, were described.

Weight factors and least squares procedures were the mathematical procedures implemented for the development of the PCR models. Additionally, statistical indicators such as RSME, MAE, R^2, and CCC were described as the main elements to assess the agreement between the historical observations and predicted PCR. Finally, implementing a confusion matrix tool would help evaluate the defined models' accuracy from a multiple PCR class perspective.

CHAPTER 4: RESULTS

This chapter comprises the obtained results from the analyzed data. First, the individual performance or distress indices models are described. Moreover, for each pavement type their proposed PCR equation is presented. Statistical indicators are analyzed to assess the agreement and concordance between the new generated PCRs and the historical observations. Cumulative distribution functions for each models' residuals are compared to defined limits by theory. Then, confusion matrices are presented and discussed to explain the PCR model accuracy for specific PCR levels.

4.1 DISTRESS SEVERITY LEVEL RATING MODELS

As explained in the methodology, the individual model definition for predominant distresses has been a dual activity in which proposed values are defined by MDOT engineers, and log-logistic models are fitted to those proposed scores. The following subsections present the indices developed for each distress or performance indicator.

4.1.1 RUTTING INDEX

A single rutting index was defined for both FLEX and COMP pavement types. Even though, these different types of pavements could have distinct structural behaviors, surface rutting has been mostly affected by traffic conditions, climate and the mixture properties when comparing both pavement types (Raffaniello et al. 2022). The values proposed by the DOT were used to fit a log-logistic model, as shown in Figure 25. The regression equation for the rutting model expressed in millimeters is also presented. Nevertheless, MDOT collects rutting depth in both International System (SI) and English units.

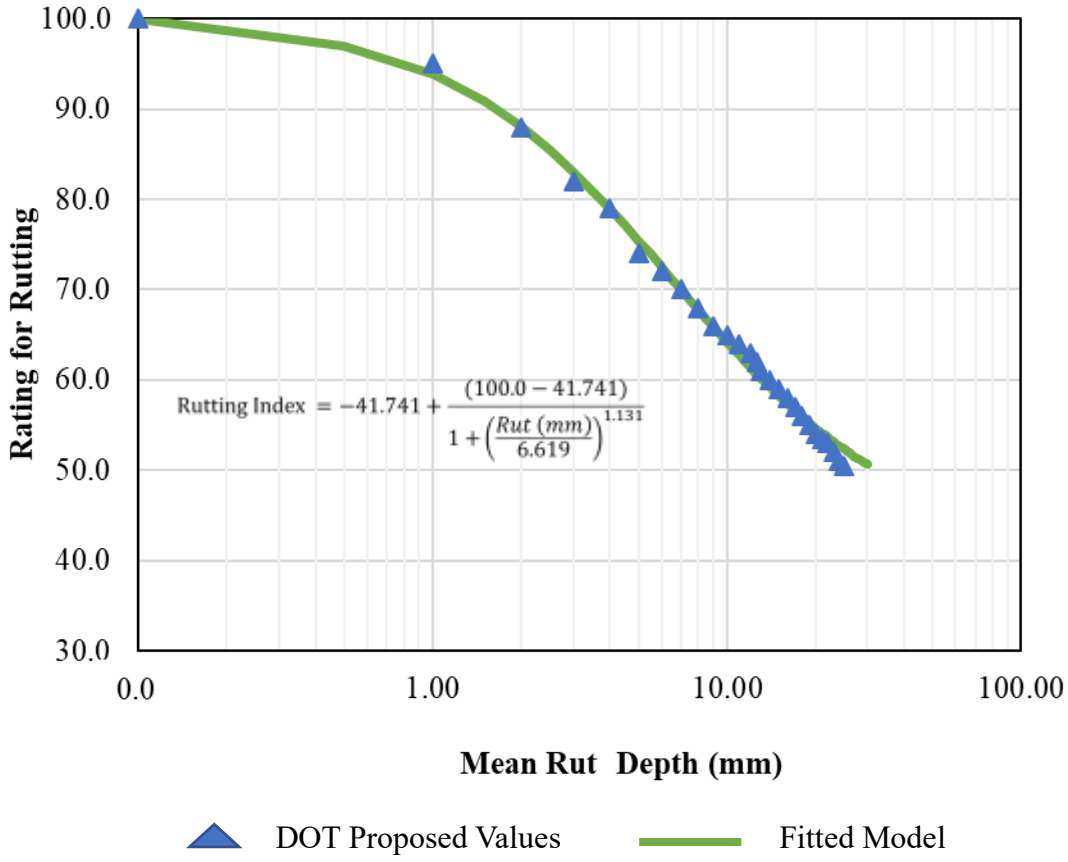

Figure 25. Rutting proposed indices and fitted model.

Table 8. Rutting index model parameters.

Parameter	Value
b	1.131
c	41.741
d	100.000
e	6.619

It is important to highlight that a residual standard error of 0.46 was obtained when the regression was fitted using R-programming. The residual standard error is utilized to measure how well a regression model fits the evaluated data, and it is expressed in the same units as the variable

analyzed (rutting index units). Therefore, it can be stated that the fitted model predicts the rutting index with an average error of 0.46 units.

4.1.2 ROUGHNESS "MRI" INDEX

Even though pavement roughness is affected by multiple factors characteristic of each pavement type (thickness, distresses experienced, subgrade type) (Elbheiry et al. 2011), MDOT has historically implemented a uniform roughness deduct value for all pavements. Therefore, as requested by MDOT, a single rutting index was defined for FLEX, COMP, JCP, and CRCP pavements. A log-logistic model was also fitted for this case, as shown in Figure 26. The model was divided into two parts, where MRI values below 20 in/mile and below result in an index of 100, while for values greater than 20 in/mile the log-logistic model is applied.

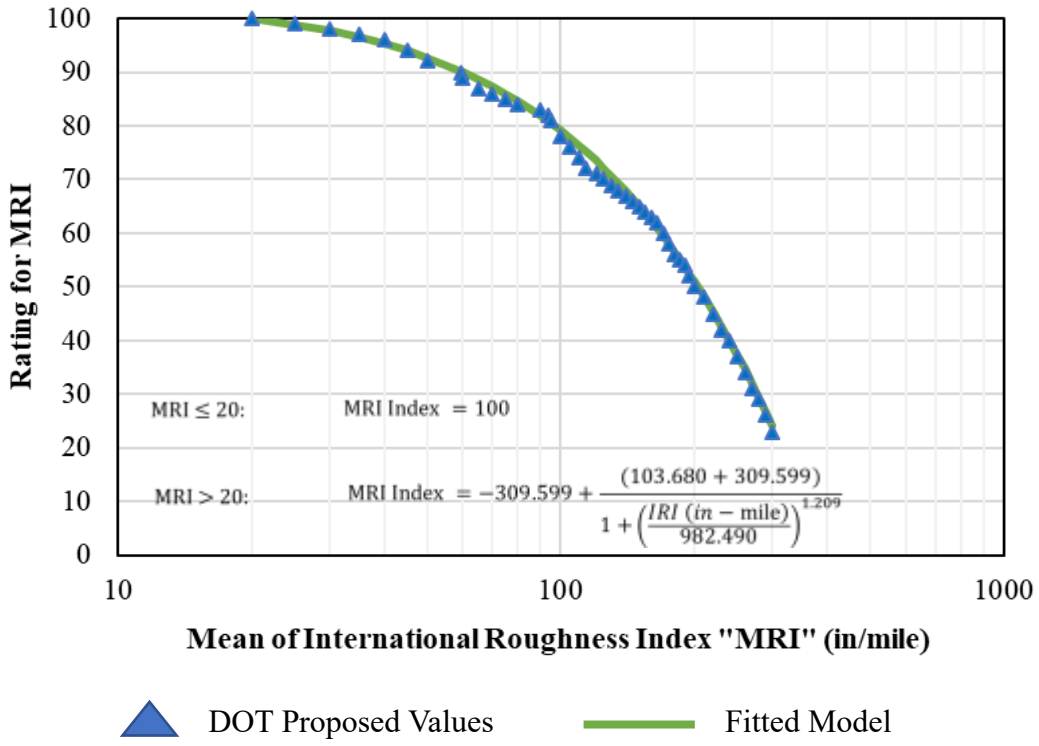

Figure 26. Roughness proposed indices and fitted model.

Table 9 summarizes the MRI model parameters. In addition, a residual standard error of 1.05 was obtained. This can be interpreted as the fitted model predicts the MRI index with an average error of 1.05 units in relation to the proposed values. A slightly greater error was obtained for this index, and it is possibly explained by the marginal differences between the proposed and regression values observed at the 100 to 130in/mile MRI range, as Figure 26 illustrates.

Table 9. MRI index model parameters.

Parameter	Value
b	1.209
c	-309.599
d	103.680
e	982.490

4.1.3 FAULTING INDEX

A faulting index model was developed for JCP pavements. Faulting measurements expressed in inches were matched to the proposed scores or indices implementing a log-logistic regression. Figure 27 illustrates the generated model compared to the data. A residual standard error of 1.18 was obtained. If compared with previous models, it could be erroneously assumed that this model is inferiorly performing due to a greater error. However, the residual standard error is dependent on the dataset dimension, so it is utilized to compare different regression models fitted to the same dataset. Table 10 summarizes the regression coefficients for the generated model.

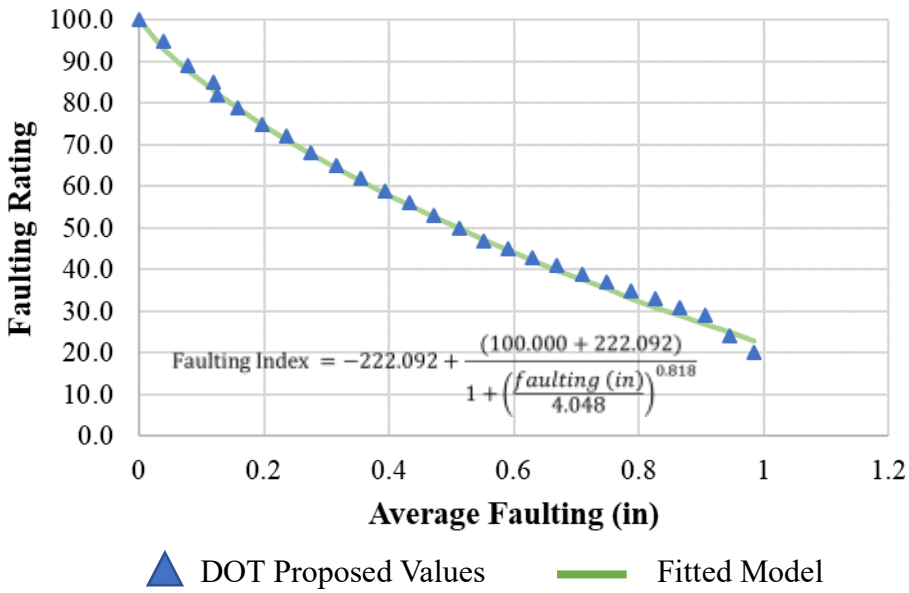

Figure 27. Faulting proposed indices and fitted model.

Table 10. Faulting index model parameters.

Parameter	Value
b	0.818
c	-222.092
d	100.000
e	4.048

4.1.4 LONGITUDINAL AND TRANSVERSE CRACKING INDEX

In terms of non-structural cracking, data is collected and classified according to three severity levels (low, medium and high severity); therefore, the generation of three independent models was needed. In contrast to the previous performance indicators or distress indices, proposed scores were not provided. Consequently, models were developed from the ground up. As explained in the methodology, non-structural cracking is analyzed using a length relation. Figure 28 illustrates the obtained models that were initially based on ASTM D-6433 deducted curves, then

revised and adjusted to meet MDOT requirements. Table 11 summarizes the model parameters for non-structural cracking.

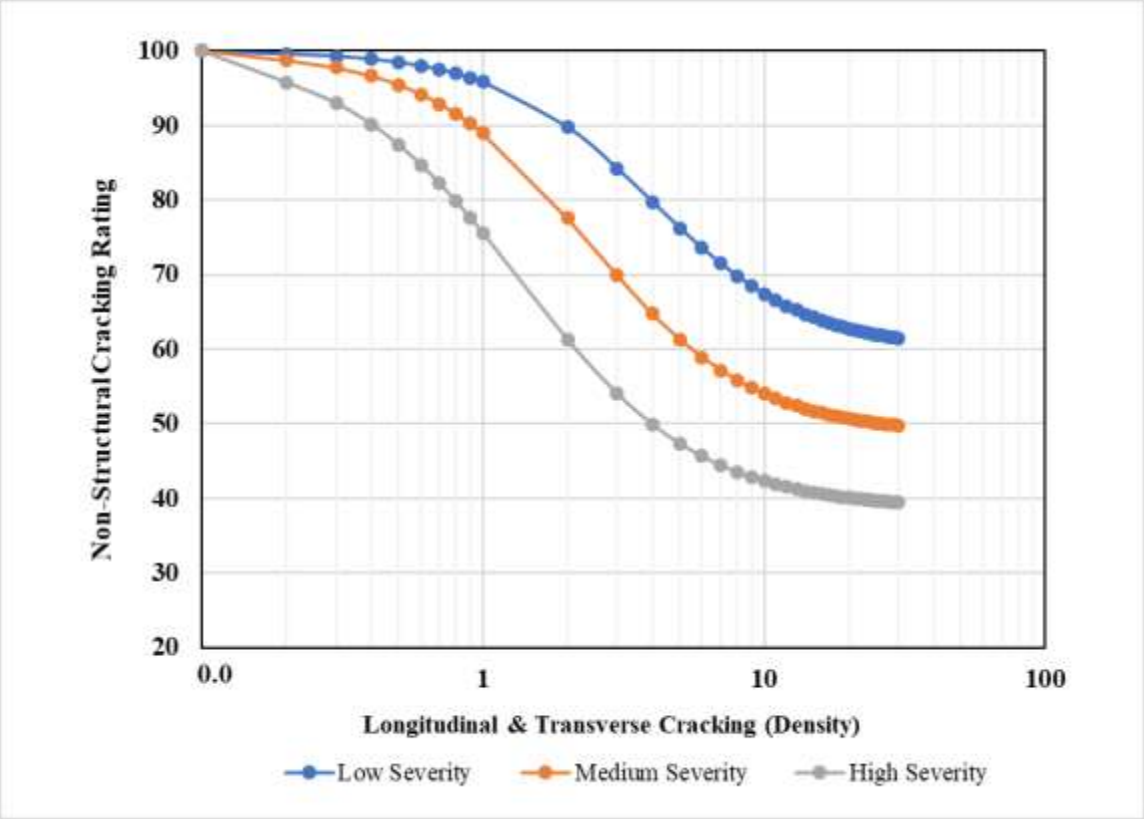

Figure 28. Non-structural cracking index model.

Table 11. Non-structural cracking index model parameters.

Parameters	Non-Structural Cracking		
	Low	Medium	High
b	1.572	1.495	1.364
c	59.907	48.662	38.568
d	100.000	100.000	100.000
e	3.945	2.376	1.352

Even though environmental factors, such as temperature and moisture, could play different roles in asphalt and concrete layers' fracture behaviors (Tang et al. 2021), a single index model for all pavement types was required by MDOT. Nevertheless, an extended study could determine

possible differences between concrete and asphalt pavements' non-structural cracking indices for equitable scoring, adjusted to structural differences between pavement types.

4.1.5 STRUCTURAL CRACKING INDEX

According to the structural cracking of FLEX pavements, a model for each severity level registered was developed. As for non-structural cracking, models were based on ASTM D-6433 deduct curves. Then they were revised and adjusted to meet MDOT requirements, since no proposed scores were directly given. For this specific case, distress density was accounted as an area relation, as explained in the methodology. Figure 29 illustrates the developed models, and Table 12 presents the obtained parameters from the non-linear regression.

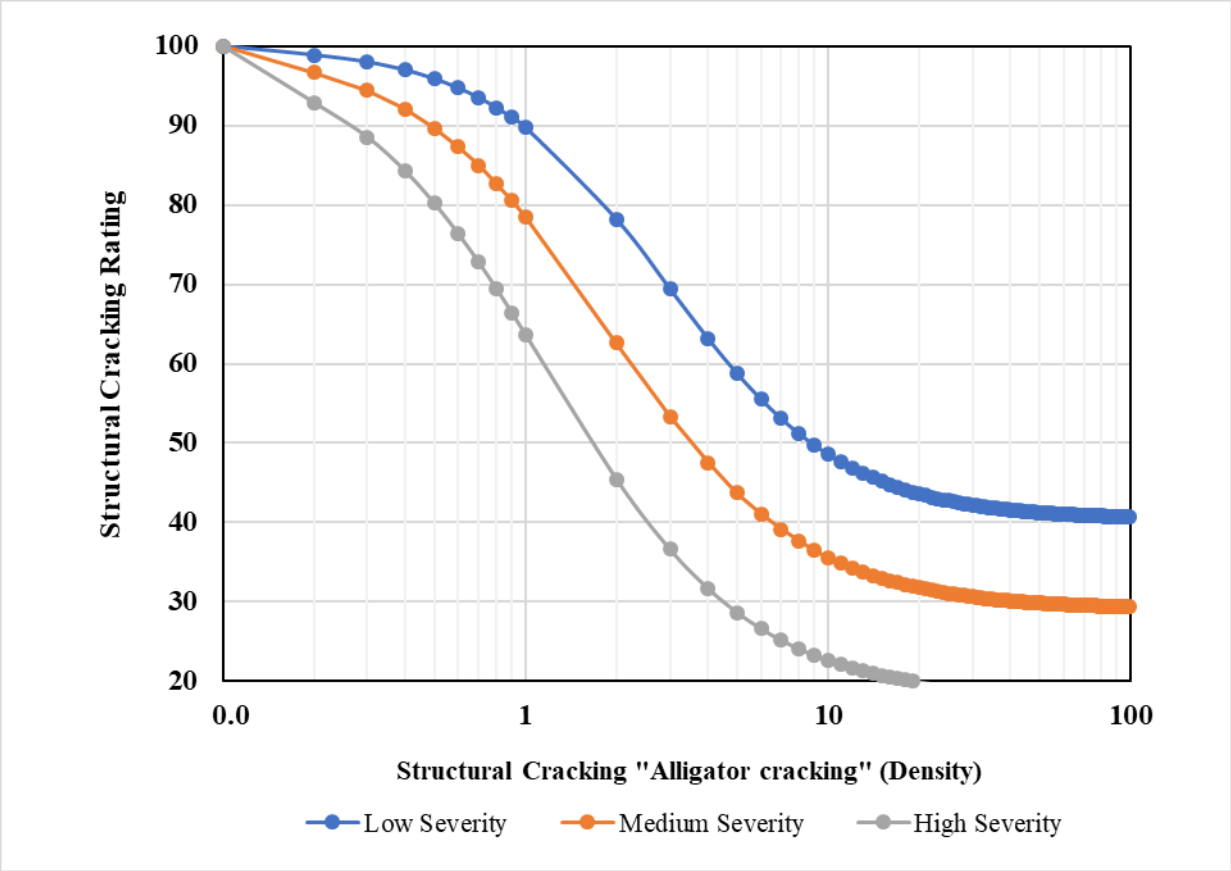

Figure 29. Structural cracking index model.

Table 12. Structural cracking index model parameters.

Parameters	Structural Cracking		
	Low	Medium	High
b	1.480	1.352	1.321
c	40.373	29.047	17.971
d	100.000	100.000	100.000
e	2.899	1.850	1.189

4.2 PCR MODELS FOR EACH PAVEMENT TYPE

After the individual indices were defined, a least squares regression was followed to quantify the weight factors of the combined PCR models. These factors not only allowed to combine each of the individual indices into a single value (PCR) but also helped to adjust PCR predictions to historical observations. Therefore, the following sections comprise the results obtained for each pavement type and the evaluation of their corresponding statistical parameters.

4.2.1 FLEX PAVEMENT PCR MODEL

Before defining the respective weight factors of the regression model, a quick check of the existing database was performed. Even though, both the contractor and MDOT filter the data as part of their QA/QC process, unusual observations were detected (IRI values below 20 in/mile, combined cracking area percentages (structural and non-structural) greater than 100%, and PCR values below 20 with discrepancies according to the distresses present). Therefore, additional filtering was performed to remove for the listed inconsistencies as discussed with MDOT. Nevertheless, data QA/QC activities executed by the contractor and agency should be revised to prevent any irregularities in future pavement assessments.

Figure 30 illustrates the comparison between the filtered and unfiltered pavement sections divided by year, in which just 2.9% of the data was discarded after filtering was applied. Therefore 97.1% of the provided dataset (52,091 observations) was used for calculating the respective weight factors. Additionally, an upward trend on the analyzed pavement sections can be also observed. It could indicate that greater portion of the pavement network is being assessed. However, it could also be that the same number of lane miles were broken into smaller pavement sections.

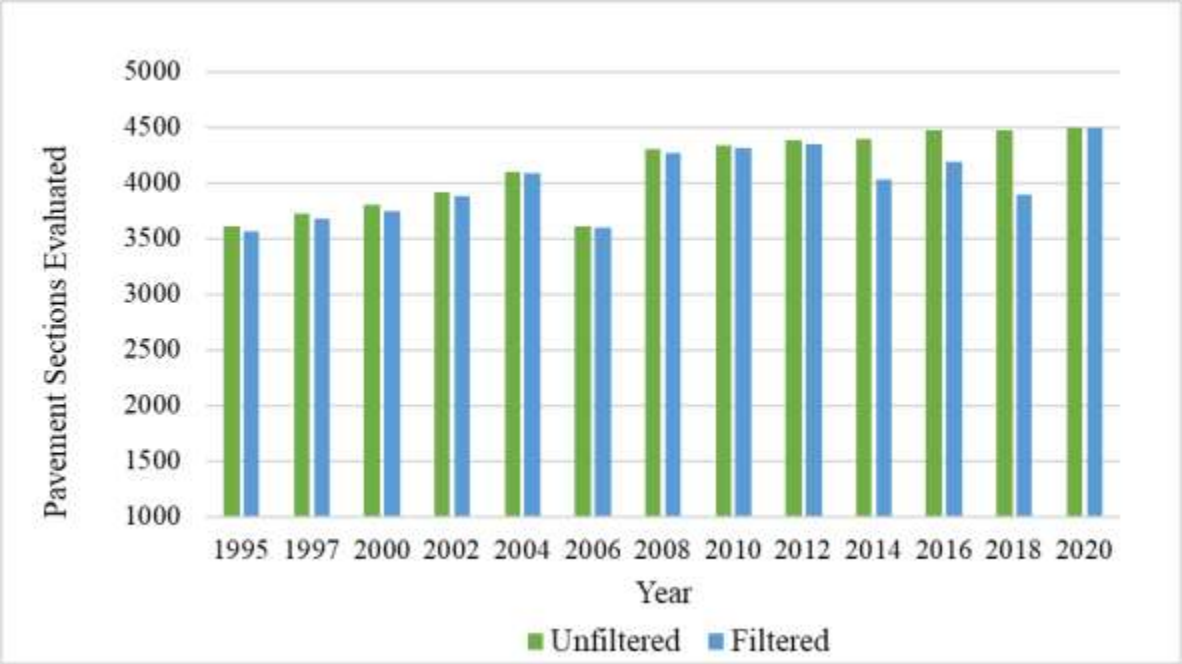

Figure 30. Analyzed flexible pavement sections.

Even though the weight factor definition depends on either a sensitivity or regression analysis, MDOT suggested some values as a preliminary starting point. The regression analysis (least of squares procedure) was performed on the training dataset, and Table 13 summarizes the coefficients (i.e. weight factors) obtained. A variation between rutting and roughness can be noticed from the suggested values. However, according to the analysis presented in Appendix 1, MRI measurements have shown the greatest correlation to historical PCR values among other

pavement performance indicators. Consequently, the adjustment of new PCRs to historical observations explains why a higher weight has been assigned to the roughness parameter.

Figure ***31*** shows the comparison between the historical PCRs (PCR by DOT) and the new calculated PCRs along the identity line, for both training and validation procedures. Preliminarily, it can be noticed that scatter increases for lower PCR values (below 60). A detailed interclass explanation is provided in further sections.

Table 13. Weight factors for FLEX pavements.

Distress/Performance Indicator	Weight Factors Suggested by DOT	Weight Factors From Regression
Rutting	0.35	0.19
Roughness "MRI"	0.25	0.56
Structural Cracking	0.25	0.15
Longitudinal and transverse cracking	0.15	0.10

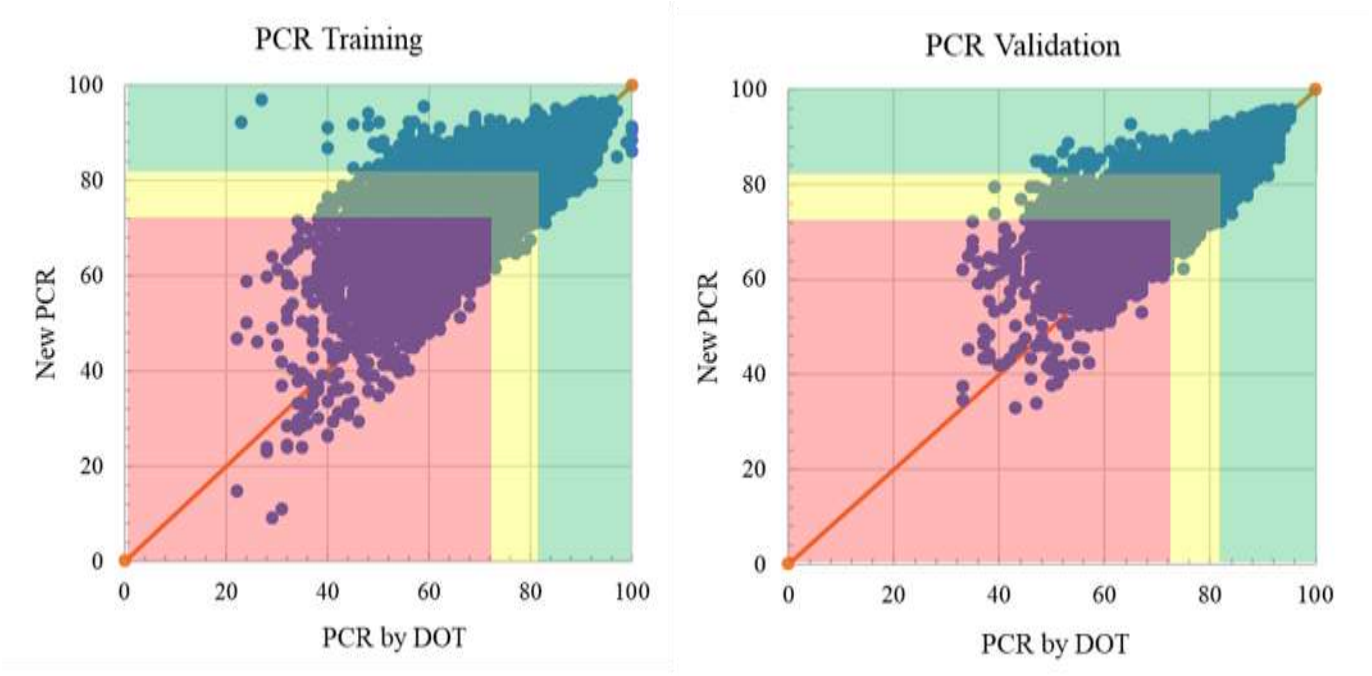

Figure 31. FLEX PCR comparison for validation and training datasets.

With the regression model developed, a statistical comparison between the predicted and historical PCRs was performed. Table 14 summarizes the obtained results. A RSME of 6.311 for the validation procedure indicates that the established model can predict PCRs with an average error of 6.311 units. However, the validation error is reduced when implementing an indicator less susceptible to outliers' effects (MAE). Despite not having a specific threshold for categorizing both indicators, lowest values are desired when comparing models (Chai and Draxler 2014). Additionally, the target of the analysis was to reduce the differences between observed and predicted PCRs as much as possible; therefore, the obtained error can be interpreted as an irreducible error.

Table 14. Average and standard deviation of statistical indicators for FLEX pavement model.

Parameter	Training		Validation	
	Average	Std. Deviation	Average	Std. Deviation
RSME	6.289	0.020	6.311	0.078
MAE	4.363	0.013	4.361	0.054
R^2	0.701	0.002	0.698	0.007
CCC	0.782	0.002	0.774	0.007

The CCC values show a strong agreement (between 0.60-0.80), if following the Pearson correlation analysis approach (Putra and Suprapto 2018). On the other hand, CCC values reveal a poor agreement if implementing the McBride (2005) approach. Nevertheless, it is important to highlight that this criterion was developed for laboratory procedures, in which testing conditions can be rigorously controlled. Therefore, translating this criterion into field measurements might be impractical due to the multiple variability associated to field testing activities (changing environmental conditions, spatial variability, etc. Consequently, the Pearson correlation approach was used on further subsections. Finally, in R^2 terms, authors have indicated that values above 0.6 indicate reasonable model accuracy for the pavement field (Timm and Turochy 2014).

4.2.2 JCP PAVEMENT PCR MODEL

The same preliminary check as for FLEX pavements was performed on the JCP database; however, no discrepancies were found. Therefore, the complete database (1,606 observations) was used for training and validation procedures. **Error! Reference source not found.** shows a r eduction on the analyzed JCP sections might guide to the idea that less JCP sections are being analyzed. However, a common M&R practice utilized by MDOT is to place asphalt overlays over existing concrete pavements, thus, changing the pavement type to COMP.

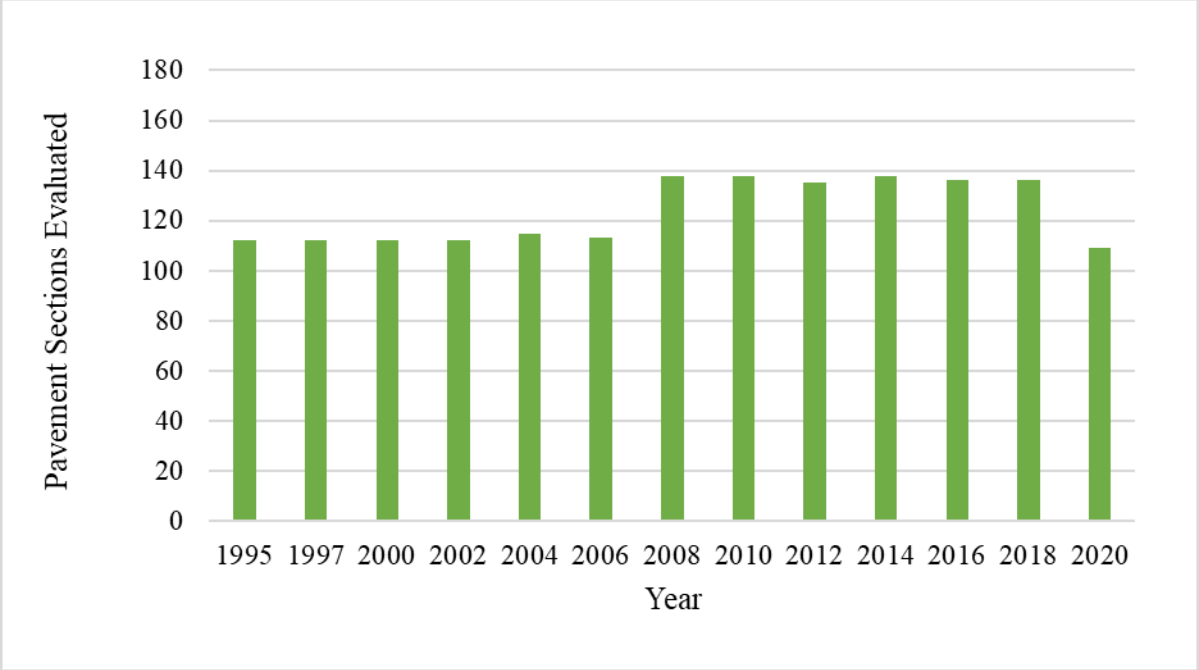

Figure 32. Analyzed jointed concrete pavement sections.

The weight factors from the regression analysis are presented in Table 15. A slight change can be noticed between roughness and faulting order from MDOT's suggestions. According to Appendix 1, roughness showed the greatest correlation to historical PCR values, and a Pearson correlation coefficient of 0.45 was obtained when comparing roughness and faulting. This result expresses a medium correlation according to the Putra and Suprapto (2018) guidelines. In other words, longitudinal profile measurements (MRI) might capture the faulting effect. Consequently,

a considerable reduction in its respective weight factor was expected. Figure 35 illustrates the comparison between the historical PCRs and new calculated PCRs along the identity line, for both training and validation procedures.

Table 15. Weight factors for JCP pavements.

Distress/Performance Indicator	Weight Factors Suggested by DOT	Weight Factors From Regression
Faulting	0.40	0.08
Roughness "MRI"	0.30	0.62
Longitudinal and transverse cracking	0.30	0.30

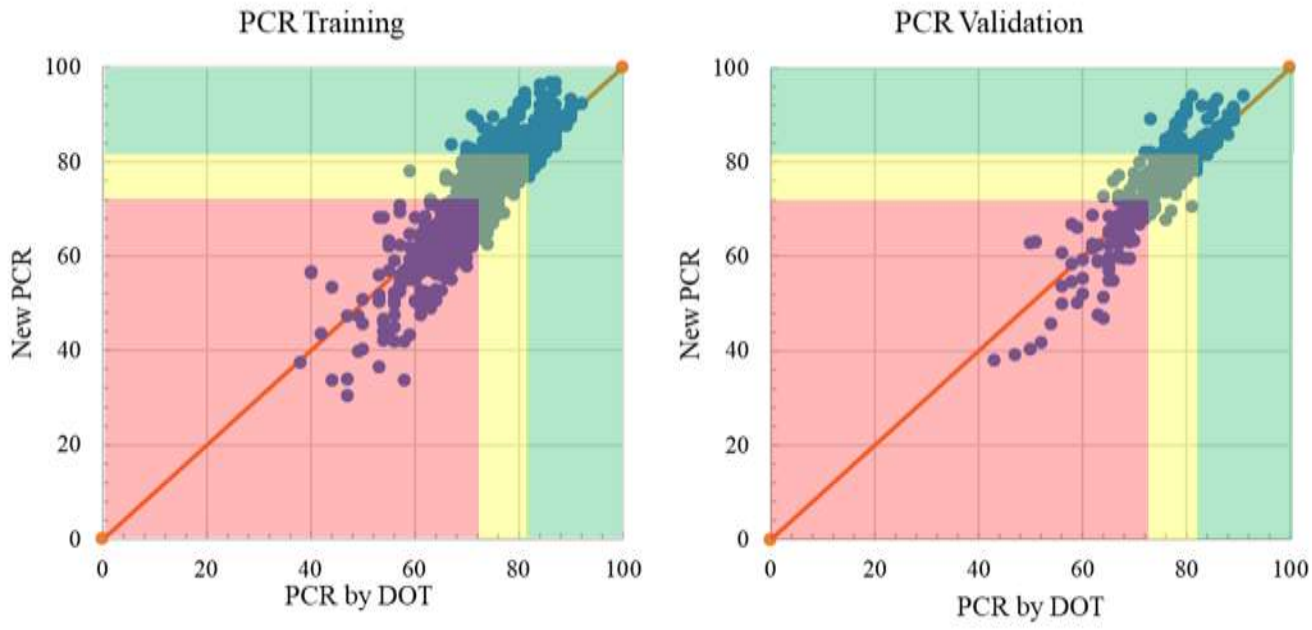

Figure 33. JCP PCR comparison for validation and training datasets.

Table 16 summarizes the statistical indicators for the JCP pavement model. Both errors (MAE and RSME) show a slight accuracy improvement if compared with the FLEX model. Additionally, CCC values reveal a very strong agreement and concordance according to Putra and Suprapto (2018) guidelines. This can also be shown in Figure 33, where the PCR values were close

to the identity line for both validation and training plots. Finally, R^2 values above 0.70 reveal the relatively high capacity of the independent variables for predicting JCP PCR values.

Table 16. Average and standard deviation of statistical indicators for JCP pavement model.

Parameter	Training		Validation	
	Average	Std. Deviation	Average	Std. Deviation
RSME	5.538	0.071	5.711	0.274
MAE	4.118	0.044	4.282	0.181
R^2	0.755	0.006	0.758	0.024
CCC	0.826	0.004	0.818	0.017

4.2.3 COMP PAVEMENT PCR MODEL

For COMP pavements just 0.45% of the data was discarded after filtering, leaving 99.5% of the provided database (14,970 observations) for training and validation procedures. Figure 34 shows the number of analyzed COMP sections. The observed increment in the analyzed COMP which is also proportional to the reduction of the JCP sections, might be a result of a common M&R practice used by MDOT (overlaying concrete pavement structures), as discussed in the previous section.

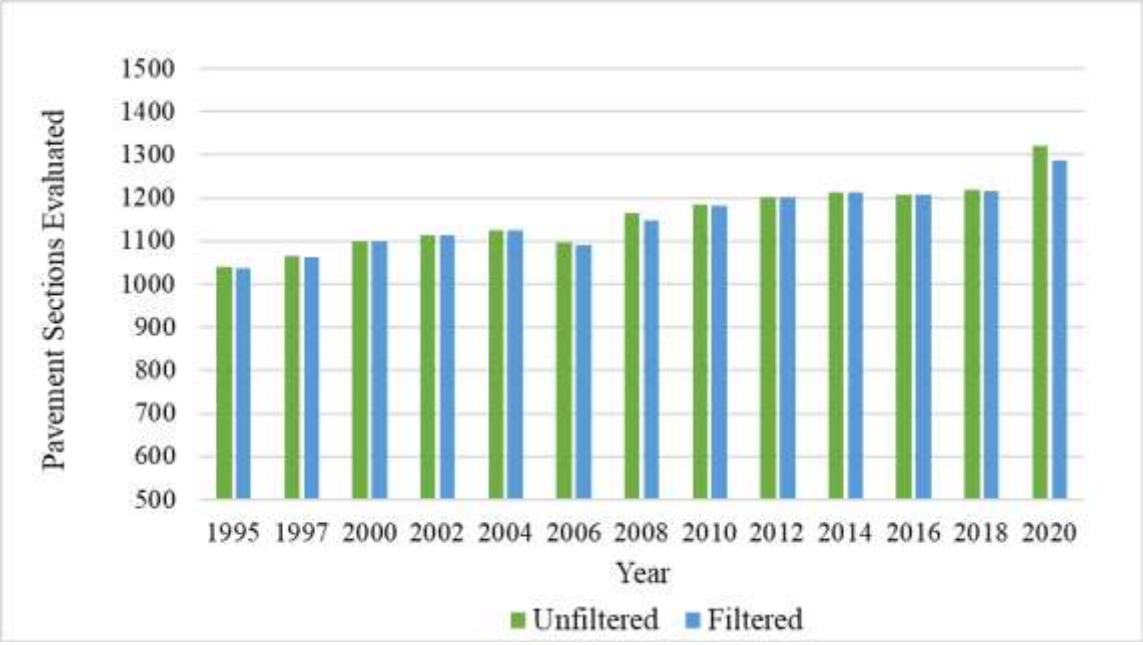

Figure 34. Analyzed composite pavement sections.

Table 17 summarizes the obtained weight factors obtained from the regression. As shown in Appendix 1, historical PCR observations for COMP pavements have also been strongly correlated to roughness measurements. Therefore, as suggested by MDOT the roughness variable presented the greatest weight factor. As illustrated by Figure 35, a similar behavior as for the flexible pavement occurs, in which scatter increases as PCR values decrease (below 65). A detailed interclass explanation and residual analysis presented in further sections will determine this effect on the model accuracy.

Table 17. Weight factors for COMP pavements.

Distress/Performance Indicator	Weight Factors Suggested by DOT	Weight Factors From Regression
Rutting	0.35	0.28
Roughness "MRI"	0.40	0.60
Longitudinal and transverse cracking	0.25	0.12

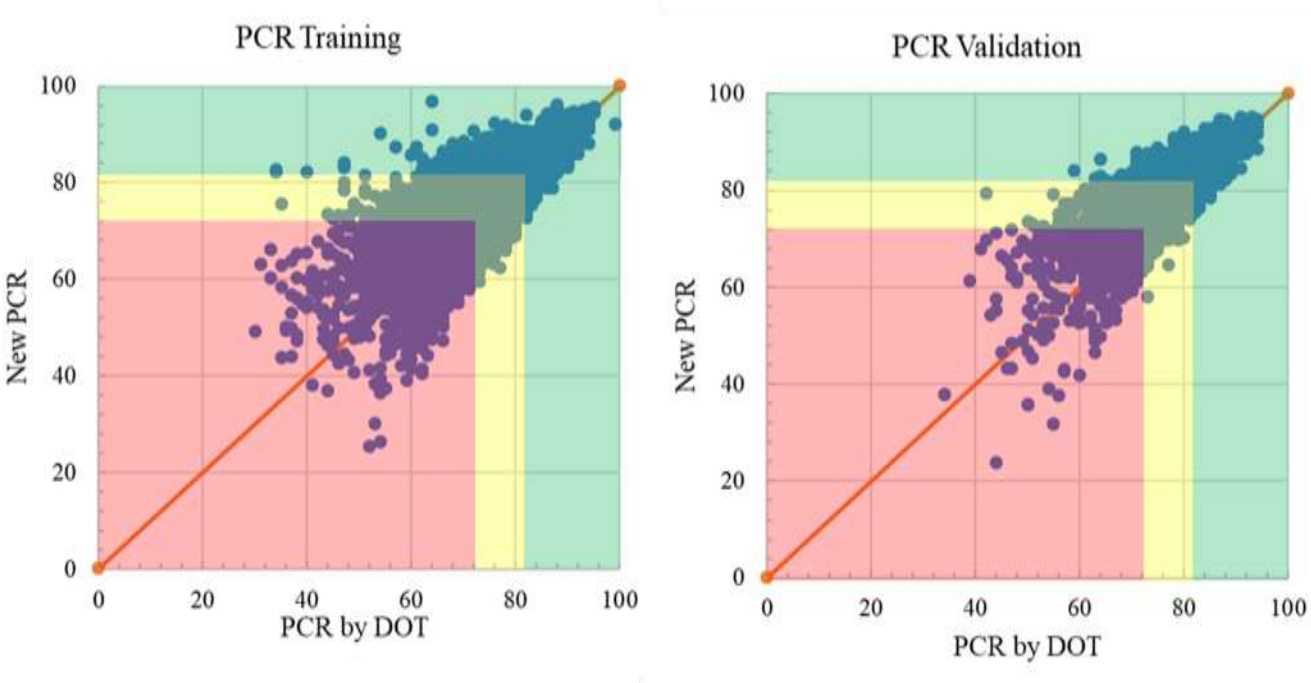

Figure 35. COMP PCR comparison for validation and training datasets.

Table 18 comprises the calculated statistical indicators for the COMP pavement model. A peculiar behavior is noted for this model, in which even though both errors (RSME and MAE) are lower than the ones for FLEX pavements, R^2 and CCC values are slightly below or almost equal to the FLEX ones. This difference can be graphically explained by Figure 35, in which for low PCR values irreducible differences are observed on both sides of the identity line (overpredicting and underpredicting). In other words, the error is distributed on both sides of the of the identity line.

Table 18. Average and standard deviation of statistical indicators for COMP pavement model.

Parameter	Training		Validation	
	Average	Std. Deviation	Average	Std. Deviation
RSME	5.901	0.017	5.959	0.068
MAE	4.321	0.016	4.354	0.066
R^2	0.673	0.001	0.667	0.005
CCC	0.789	0.001	0.786	0.004

4.2.4 CRCP PAVEMENT PCR MODEL

After performing a preliminary check on the CRCP database, no discrepancies were found. Therefore, the entire database (845 observations) was used for training and validation procedures. Figure 36 illustrates the progression of the analyzed sections. A similar trend as for JCP pavements was discovered, in which for recent years concrete pavement sections started to decrease.

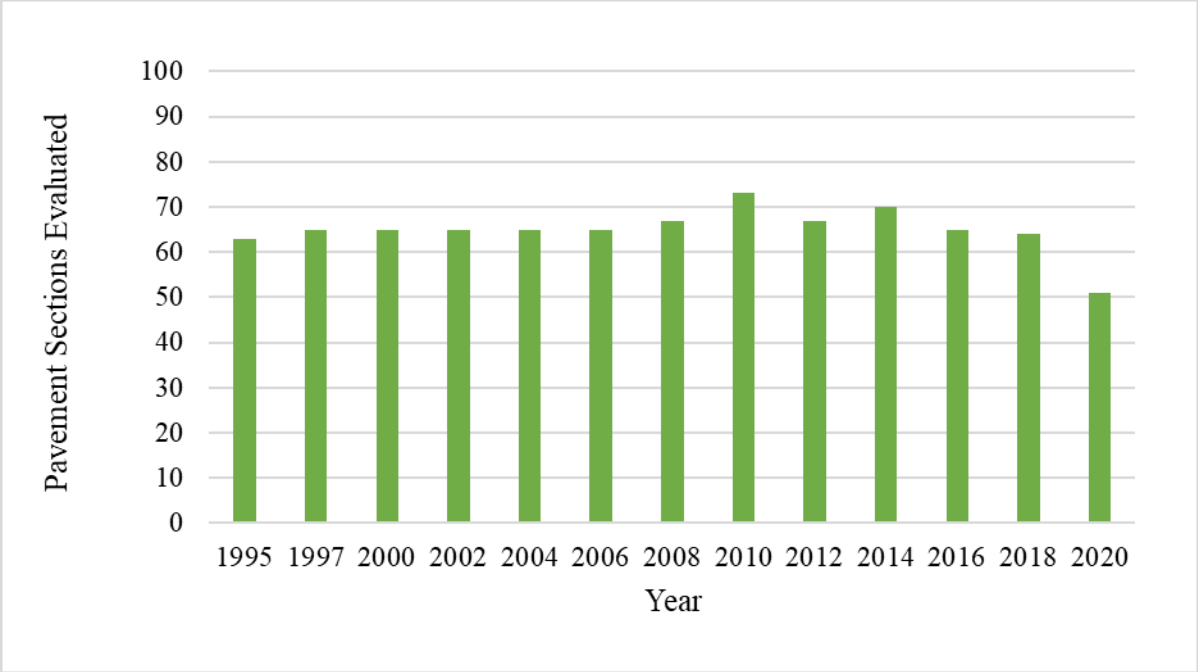

Figure 36. Analyzed continuously reinforced concrete pavement sections.

The weight factors obtained from the least of squares procedure are presented in Table 19. As expected from the CRCP historical observations shown in Appendix 1, PCR values revealed very strong correlation with IRI measurements. Therefore, to adjust the new PCR values to historical trends, MRI measurements exhibited the greatest weight. Figure 37 illustrates the comparison between calculated and historical PCRs for both training and validation processes, in which a preliminary good adjustment along the identity line is graphically observed.

Table 19. Weight factors for CRCP pavements.

Distress/Performance Indicator	Weight Factors Suggested by DOT	Weight Factors From Regression
Roughness "MRI"	0.50	0.67
Longitudinal and transverse cracking	0.50	0.33

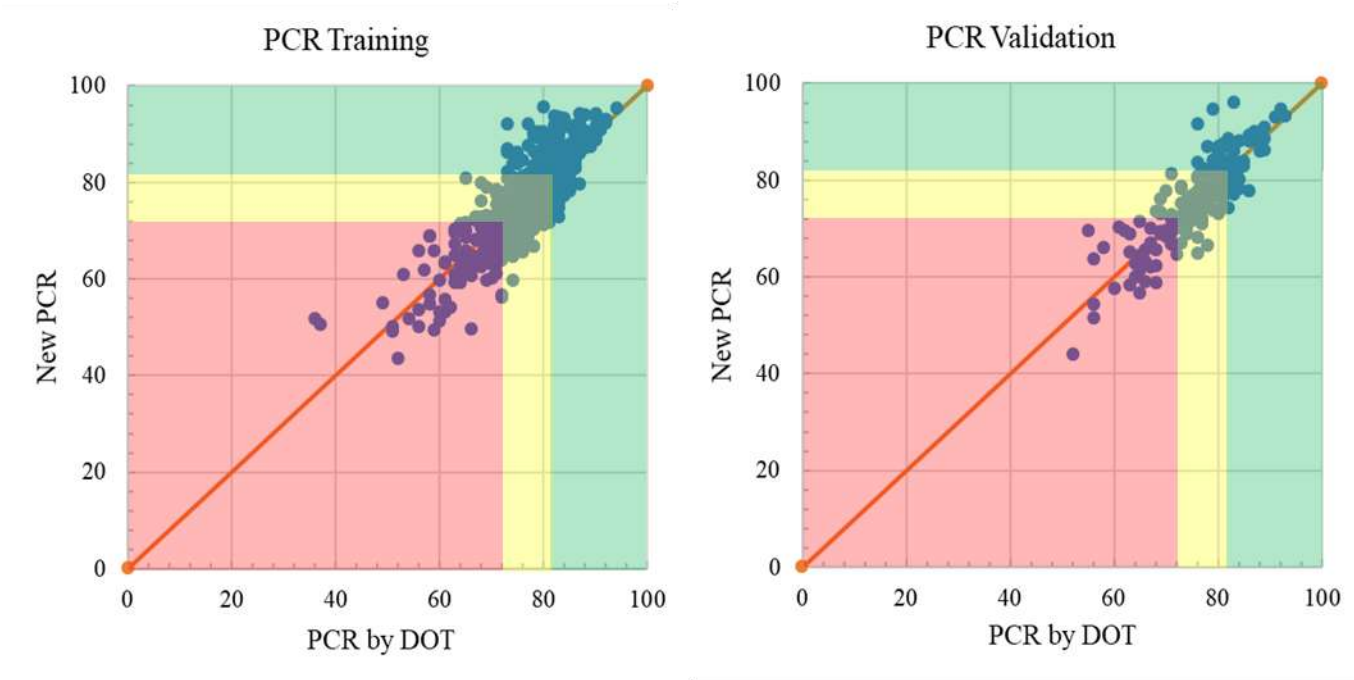

Figure 37. CRCP PCR comparison for validation and training datasets.

Even though CRCP database comprised the lowest number of analyzed pavement sections, it presented the lowest errors when compared to the other pavement PCR models, as shown in Table 20. In addition, obtained CCC values reveal a very strong agreement and concordance (above 0.80) between historical a new calculated PCRs according to the Putra and Suprapto (2018) guidelines. Finally, a R^2 above 0.6 reveals a reasonable capacity of the independent variables to explain the CRCP PCRs according to Timm and Turochy (Timm and Turochy 2014).recommendations.

Table 20. Average and standard deviation of statistical indicators for CRCP pavement model.

Parameter	Training		Validation	
	Average	Std. Deviation	Average	Std. Deviation
RSME	4.962	0.070	4.794	0.296
MAE	3.789	0.057	3.871	0.226
R2	0.694	0.012	0.691	0.050
CCC	0.819	0.008	0.819	0.035

4.3 MODEL RESIDUALS AND CONFUSION MATRICES

In order to assess the differences between the actual method for determining PCRs and the proposed method in this document, residuals were analyzed following practical limits proposed by Timm and Turochy (2014). Specifically, different practical limits (±10 and ±5 PCR units) were implemented when comparing vendor-computed PCR values and PCR values defined by the Alabama Department of Transportation (ALDOT) residuals. Due to the similarities between studies this approach was selected for evaluating the described differences.

Figure 38 illustrates the validation residuals as a cumulative distribution for each pavement type for one of the iterations. It is possible to observe that most of the data is within the ±10 practical range, and a considerable portion is within the ±5 range. A similar distribution between COMP and FLEX pavements was revealed, this could explain the similarity between their respective errors presented in previous sections. Timm and Turochy (2014) concluded that for pavement M&R prioritizing procedures an 84.1% of the data within the ±10 range was considered sufficiently accurate. Therefore, if looking at the results presented in Table 21, more than 90% of the residuals were within the ±10 range for all pavement types, even when more data was analyzed. This reaffirms the accuracy and adjustment of the developed models. Furthermore, an strict criteria is presented on the ASTM D-6433 standard, in which the acceptable error for estimating a pavement section PCI ranges between ±5 PCI units (ASTM 2020b). For this study over 70% of the predicted PCRs were within that range.

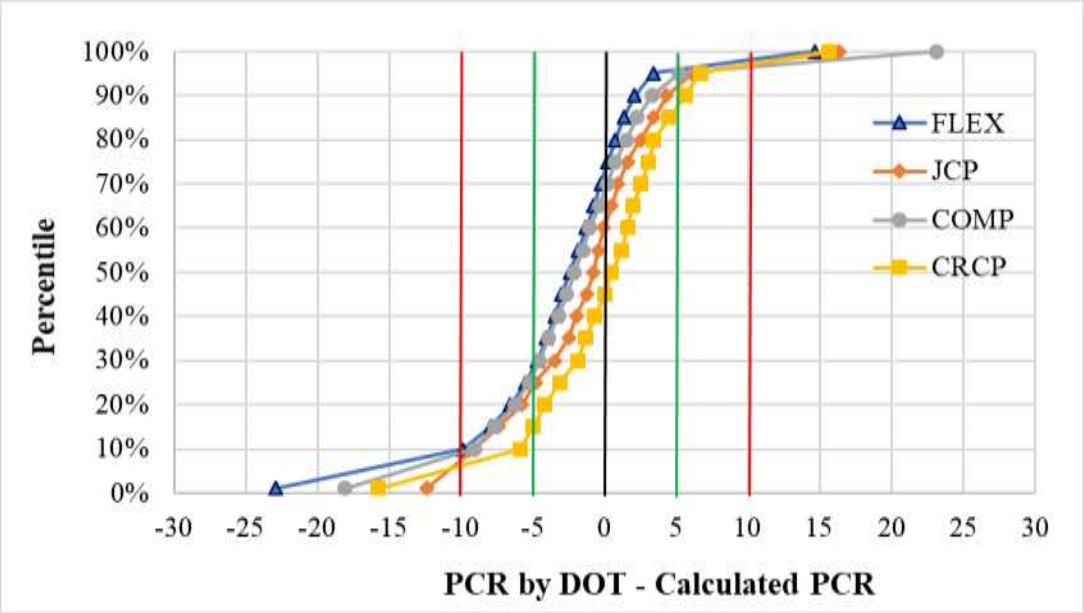

Figure 38. Cumulative Residual Distribution.

Table 21. Average percentage of PCR residuals within practical limits.

Practical Limit	Parameter	PCR residuals within limits (%)			
		FLEX	JCP	COMP	CRCP
±5.0	Average	69.7	69.0	67.9	72.1
	Standard Deviation	0.9	1.3	1.1	4.8
±10.0	Average	90.2	90.3	90.9	96.7
	Standard Deviation	0.5	0.9	0.3	0.8

Even though the residual analysis indicates an adequate accuracy for the presented models, it is important to assess the respective interclass performance, since one of the fundamental model's objectives is to predict PCR in the correct category (good, fair or poor). In contrast to correlation measurements and descriptive statistical methods, a confusion matrix can reveal how incorrect predictions are distributed into other categories (Provost and Fawcett 2013; Piryonesi and El-Diraby 2018). For this reason, this tool was implemented in the validation datasets.

As shown in Figure 39, the four confusion matrixes present the models' observations for one validation cycle. Specifically, for both FLEX and COMP models an acceptable class precision

was observed. However, when focusing on the class recall a lowest number was observed for the "poor" category, indicating that actual (historical observations) sections classified as "poor" have been categorized by the new model as "fair", and in some cases even as "good". From a numerical perspective, this difference in class recalls could be caused by a greater portion of the data in the good and fair range with lower variations, therefore the regression would focus on reducing the differences in that range. For instance, for the FLEX pavement database the poor category presented the lowest number of observations, with just 21% of the entire database.

On the other hand, concrete pavements mostly show a higher class recall and precision as pavement condition decreases. This could be also explained by a greater portion of the data in the lower and intermediate ranges that the regression is focusing to adjust. For instance, when analyzing the JCP pavement database just 17.0% of the sections were in good category. Additionally, this effect would be correlated with the premise that concrete pavements have been transformed into composite pavements due to the typical application of an asphalt overlay as a M&R technique.

Even though PCR models have shown some interclass differences when comparing historical observations and predicted values, they are going to be implemented for predicting PCR from new collected data. Nevertheless, a deeper analysis that considers the proposed indices by MDOT, the distress distributions for each specific class, and the PCR occurrences per year and category would be an ideal tool for further calibration. Furthermore, the analysis of the specific models' accuracy is going to give a clear perspective of their overall performance. **Table *22.*** Average calculated model accuracy.Table 22 presents the average and one standard deviation of the obtained accuracy for each model. It can be noted that on average, approximately 65-70% of predictions were correct. For instance, if compared with similar studies, Piryonesi and El-Diraby

(2018) reported a model accuracy of 69.2 ± 4.7 percent for their specific conditions, a close value to the one obtained in the present study. Additionally, as data becomes available further calibrations can be done, and the model's ability to predict unseen data can be enhanced.

FLEX Pavement

Predicted /Actual PCR	Actual Good	Actual Fair	Actual Poor	Class Precision
Predicted Good	3241	1060	138	73.0%
Predicted Fair	246	2635	1253	63.7%
Predicted Poor	0	225	1616	87.8%
Class Recall	92.9%	67.2%	53.7%	-

JCP Pavement

Predicted /Actual PCR	Actual Good	Actual Fair	Actual Poor	Class Precision
Predicted Good	40	53	1	42.6%
Predicted Fair	7	102	10	85.7%
Predicted Poor		14	93	86.9%
Class Recall	85.1%	60.4%	89.4%	-

COMP Pavement

Predicted /Actual PCR	Actual Good	Actual Fair	Actual Poor	Class Precision
Predicted Good	765	292	22	70.9%
Predicted Fair	70	789	376	63.9%
Predicted Poor	0	151	530	77.8%
Class Recall	91.6%	64.0%	57.1%	-

CRCP Pavement

Predicted /Actual PCR	Actual Good	Actual Fair	Actual Poor	Class Precision
Predicted Good	23	20	0	53.5%
Predicted Fair	18	51	9	65.4%
Predicted Poor	0	17	27	61.4%
Class Recall	56.1%	58.0%	75.0%	-

Figure 39. Confusion matrix for each pavement model.

Table 22. Average calculated model accuracy.

Parameter	Model Accuracy (%)			
	FLEX	JCP	COMP	CRCP
Average	71.4	69.7	70.6	65.2
Standard Deviation	0.3	1.9	0.8	3.5

4.4 SUMMARY

The present chapter comprises the main results obtained from the analysis process performed on the given databases. Initially, performance indicator models were developed based on sigmoidal functions (log-logistic function) and suggested values by MDOT. These models allowed to correlate a distress density to a specific score or index. Furthermore, with the indices defined, a least squared regression analysis was performed to assign a weight to each predominant distress (represented by their respective index), and to adjust to historical observations. From this process, it was found that roughness measurements govern the PCR. Specifically, weight factors between 0.56 and 0.67 imply that 56% to 67% of the pavement PCR is explained by the roughness effect. In addition, other distresses such as faulting have been reflected in this longitudinal profile measurement.

Statistical indicators as CCC indicate that predicted values from regression models show a strong to very strong correlation according to the Pearson coefficient approach. A residual analysis revealed that more than 90% of the residuals were within the ±10 PCR range for all pavement types, indicating an adequate model performance for predicting PCRs. Finally, confusion matrices indicated that PCR models can accurately predict between 65% to 70% of the unseen data.

CHAPTER 5: CONCLUSIONS AND RECOMMENDATIONS

The primary objective of this research was to generate a method for calculating MDOT pavement condition ratings and adjusting them to historical observations in order to reflect continuity in the rating system. An individual index method and a least squares regression procedure were conducted using data biannually collected from 1995 to 2020. In relation to the present research, the following conclusions and recommendations are drawn:

5.1 CONCLUSIONS

- In conclusion it was found that sigmoidal log-logistic functions accurately represent MDOT-suggested deterioration indices with residual standard errors that ranged between 0.46 to 1.18 PCR units.
- From the least square regression analysis and as expected from the historical observations, it can be concluded that the predicted PCRs were mostly driven by the effect of pavement roughness, which presented the greatest weight factors in the new PCR calculation method and the highest correlations with historical PCRs values.
- For the JCP pavement model, a medium statistically significant correlation between roughness measurements (MRI values) and faulting was found. It can be concluded that the effect of the elevation difference between adjacent slabs is captured by the longitudinal profile measurements.
- On synthesis, a strong to a very strong agreement was found between the predicted and historical PCRs by following the Pearson correlation analysis approach of CCC values. It indicates that the combined effect of both distress list reduction and the establishment of a

new PCR calculation method marginally impacts historical PCR trends, which was also reflected in a greater portion of the PCR residuals within the practical limits analyzed.

- It can be concluded that even by reducing the predominant distress list and passing to a simplified PCR calculation method, the developed models can accurately predict between 65% to 70% of the unseen data; an acceptable precision for pavement categorizing applications when compared to similar studies. Nevertheless, as data becomes available and further calibrations are performed; overall accuracy can be improved.

5.2 RECOMMENDATIONS

- After the proposed PCR calculation method is implemented, it is recommended to continue assessing the distress distributions and possible outliers in the collected data. Therefore, a double check in data QA/QC procedures from both contractor and MDOT sides, can improve data quality process, and prevent having additional data filtering processes.
- It is recommended to perform a more in-depth analysis that considers the proposed indices by MDOT, the multiple distresses distributions for each specific class, and the PCR occurrences per year and category would be an ideal tool for further calibration.
- It is recommended to evaluate alternative data splitting methods as random stratified or cross-validation procedures for each individual pavement dataset, to determine if there exist statistically significant differences in model training and validation procedures derived from the data partition methods.

REFERENCES

Altman, D. G. (1991). *Practical Statistics for Medical Research*. CRC Press.

American Association of State Highway and Transportation Officials (AASHTO)). (2017). *Standard Practice for Quantifying Cracks in Asphalt Pavement Surfaces from Collected Pavement Images Utilizing Automated Methods*.

American Society of Testing Materials (ASTM). (2020a). *ASTM E867: Standard Terminology Relating to Vehicle-Pavement Systems*.

American Society of Testing Materials (ASTM). (2020b). *ASTM D6433: Standard Practice for Roads and Parking Lots Pavement Condition Index Surveys*.

Attoh-Okine, N., and Adarkwa O. (2013). "Pavement condition surveys–overview of current practices." *Del. Cent. Transp. Univ. Del. Newark USA*.

Ayers, M., Cackler, T., Fick, G., Harrington, D., Schwartz, D., Smith, K, Snyder, M., and Van Dam, T. (2018). "Guide for Concrete Pavement Distress Assessments and Solutions: Identification, Causes, Prevention, and Repair."

Bektas, F., Smadi, O., and Al-Zoubi, M. (2014). *Pavement Management Performance Modeling: Evaluating the Existing PCI Equations*. Institute for Transportation Iowa State University.

Carey, W., and Irick, P. (1960). "The Pavement Serviceability-Performance Concept." *Highw. Res. Board Bull.*, (250).

Chai, T., and Draxler, R. (2014). "Root mean square error (RMSE) or mean absolute error (MAE)?" *Geosci Model Dev*, 7. https://doi.org/10.5194/gmdd-7-1525-2014.

Choi, P., L. Poudyal, F. Rouzmehr, and M. Won. (2020). "Spalling in Continuously Reinforced Concrete Pavement in Texas." *Transp. Res. Rec.*, 2674 (11): 731–740. SAGE Publications Inc. https://doi.org/10.1177/0361198120948509.

Chowdari, S. (2019). *MDOT PMS Update Report August 2019*. Unpublished manuscript.

City and County Pavement Improvement Center. (2021). *Pavement Condition Index (PCI) There is more (and less) to the Score*. University of California.

Concrete Reinforcing Steel Institute. (2001). *Summary of CRCP Design and Constructions Practices in the U.S*.

DeSantis, J., Sachs, S., and Vandenbossche, J. (2020). "Faulting development in concrete pavements and overlays." *Int. J. Pavement Eng.*, 21 (12): 1445–1460. Taylor & Francis. https://doi.org/10.1080/10298436.2018.1548706.

Duncan, G. M., L. V. Sibaja Vargas, P. Ram, K. A. Zimmerman, Inc. Applied Pavement Technology, and Mississippi. Dept. of Transportation. (2017). *Development of a Pavement Management Manual and Data Quality Plan for the Mississippi Department of Transportation*.

Elbheiry, M. R., K. A. Kandil, and A. S. Kotb. (2011). "Investigation of factors affecting pavement roughness." *Eng. Res. J.*, 132.

Elhadidy, A., El-Badawy, S., and Elbeltagi, E. (2021). "A simplified pavement condition index regression model for pavement evaluation." *Int. J. Pavement Eng.*, 22 (5): 643–652. Taylor & Francis. https://doi.org/10.1080/10298436.2019.1633579.

Federal Highway Administration. (2016). *Measuring and Specifying Pavement Smoothness*. Tech Brief.

Filho, D., Júnior,J., and.Rocha, E. (2011). "What is R2 all about?" *Leviathan São Paulo*, (3): 60–68. https://doi.org/10.11606/issn.2237-4485.lev.2011.132282.

Flintsch, G., Diefenderfer, B., Nunez, O. (2008). *Composite pavement systems: synthesis of design and construction practices.* Virginia Transportation Research Council, Virginia. Dept. of Transportation, and United States. Federal Highway Administration.

Finn, F. (1998). "Pavement Management Systems - Past, Present, and Future, Public Roads: 80 Years Old, But The Best Is Yet to Come." *Public Roads*, 62 (1).

George, K. P. (2000). *MDOT Pavement Management System : Prediction Models and Feedback System*. University of Mississippi. Dept. of Civil Engineering.

Gharaibeh, G., Zou, Y., and Saliminejad, S. (2010). "Assessing the Agreement among Pavement Condition Indexes." *J. Transp. Eng.*, 136 (8): 765–772. American Society of Civil Engineers. https://doi.org/10.1061/(ASCE)TE.1943-5436.0000141.

Gossman A. (2020). "Concordance Correlation Coefficient." *0-Fold Cross-Valid.* https://www.alexejgossmann.com/ccc/.

Haas, R., Hudson, W., and Zaniewski, J. (1994). *Modern Pavement Management*. https://trid.trb.org/view/388787

Hasan, O., Ziyadi, M., and Feng, Y. (2018). *Revised Condition Rating Survey Models. To Reflect Pavement Distresses: Volume 1*. Illinois Center for Transportation.

Huang, Y. H. (2004). *Pavement analysis and design*. Upper Saddle River, NJ: Pearson/Prentice Hall.

Jeon, S., Choi, P., and Won, M. (2021). "Punchout evaluations and classification of continuously reinforced concrete pavement to improve pavement design." *Road Mater. Pavement Des.*, 22 (7): 1481–1499. Taylor & Francis. https://doi.org/10.1080/14680629.2019.1701538.

Kulkarni, R., and Miller, R. (2002). "Pavement Management Systems: Past, Present, and Future." *Transp. Res. Rec.*, 1853. https://doi.org/10.3141/1853-08.

Kumar, P., and Gupta, A. (2010). "Case Studies on Failure of Bituminous Pavements."

Lin, L. I. (1989). "A concordance correlation coefficient to evaluate reproducibility." *Biometrics*, 45 (1): 255–268.

Llopis-Castelló, D., García-Segura, T., Montalbán-Domingo, L., Sanz, A., and Pellicer, E. (2020). "Influence of Pavement Structure, Traffic, and Weather on Urban Flexible Pavement Deterioration." *Sustainability*, 12: 9717. https://doi.org/10.3390/su12229717.

Louisiana Department of Transportation. (2021). *Louisiana DOTD Pavement Data Quality Management Program*.

Mackiewicz, P. (2018). "Fatigue cracking in road pavement." *IOP Conf. Ser. Mater. Sci. Eng.*, 356: 012014. https://doi.org/10.1088/1757-899X/356/1/012014.

McBride G. (2005). *A Proposal for Strength-of-Agreement Criteria for Lin's Concordance Correlation Coefficient*.

McGhee, K. (2002). *Development and Implementation of Pavement Condition Indices for the Virginia Department of Transportation*.

Menendez, J. (2014). *Incorporating Risk and Uncertainty into Pavement Network Maintenance and Rehabilitation Budget Allocation Decisions*. https://www.medcalc.org/download/pdf/McBride2005.pdf

Merritt, D.., Chang, G., Rutledge, L., and Inc. Transtec Group. (2015). *Best practices for achieving and measuring pavement smoothness, a synthesis of state-of-practice. https://rosap.ntl.bts.gov/view/dot/28837*

Miller, J., and Bellinger, W. (2014). *Distress Identification Manual for the Long-Term Pavement Performance Program (Fifth Revised Edition)*. Federal Highway Administration (FHWA).

Mississippi. Dept. of Transportation. (2022). *MDOT State-Maintained Road Network by County - Average Pavement Condition Rating (PCR) history by year*.

National Institute of Standards and Technology. (2012). "Least Squares." *Eng. Stat. Handb.*

Norouzi, A., and Kim, R. (2017). "Mechanistic evaluation of fatigue cracking in asphalt pavements." *Int. J. Pavement Eng.*, 18 (6): 530–546. Taylor & Francis. https://doi.org/10.1080/10298436.2015.1095909.

Onofri, A. (2019). "Some useful equations for nonlinear regression in R." https://www.statforbiology.com/nonlinearregression/usefulequations#log-logistic_curve.

Pathway Services Inc. (2016). *MDOT Distress Classification Guide*.

Papagiannakis, A., Gharaibeh, N., Weissmann,J., and Wimsatt.A. (2009). *Pavement Scores Synthesis*. Texas Transportation Institute The Texas A&M University System.

Piryonesi, M., and El-Diraby, T. (2018). "Using Data Analytics for Cost-Effective Prediction of Road Conditions: Case of The Pavement Condition Index." Federal Highway Administration.

Provost, F and Fawcett, T. (2013). *Data Science for Business: What You Need to Know About Data Mining and Data-Analytic Thinking*. O'Reilly Media.

Putra, D. A., and Suprapto, M. (2018). "Assessment of the road based on PCI and IRI roadroid measurement." *MATEC Web Conf.*, 195: 04006. EDP Sciences. https://doi.org/10.1051/matecconf/201819504006.

Raffaniello, A., Bauer, M., Safiuddin, M., and El-Hakim, M. (2022). "Traffic and Climate Impacts on Rutting and Thermal Cracking in Flexible and Composite Pavements." *Infrastructures*, 7 (8): 100. Multidisciplinary Digital Publishing Institute. https://doi.org/10.3390/infrastructures7080100.

Roesler, J., Hiller, J., and Brand, A. (2016). *Continuously Reinforced Concrete Pavement Manual Guidelines for Design, Construction, Maintenance, and Rehabilitation*. Federal Highway Administration (FHWA).

Roshan, J. (2022). "Optimal ratio for data splitting." *Stat. Anal. Data Min. ASA Data Sci. J.*, 15 (4): 531–538. https://doi.org/10.1002/sam.11583.

Sarsam, S. (2016). "Pavement Maintenance Management System: A Review." *Trends Transp. Eng. Appl.*, 3: 19–30.

Shahin, M., and Kohn, S. (1979). “Development of a Pavement Condition Rating Procedure for Roads, Streets, and Parking Lots. Volume ii. Distress identification manual.”

Shahin, M. (2005). *Pavement Management for Airports, Roads, and Parking Lots*.

Shahnazari, H., Tutunchian, M., Mashayekhi, M., and Amini, A. (2012). “Application of Soft Computing for Prediction of Pavement Condition Index.” *J. Transp. Eng.*, 138: 1495–1506. https://doi.org/10.1061/(ASCE)TE.1943-5436.0000454.

Shtayat, A., Moridpour, S., Best, B., and Rumi, S. (2022). “An Overview of Pavement Degradation Prediction Models”. *Journal of Advanced Transportation*. https://doi.org/10.1155/2022/7783588.

Simpson, A.. (1999). “Characterization of Transverse Profile.” *Transp. Res. Rec.*, 1655 (1): 185–191. SAGE Publications Inc. https://doi.org/10.3141/1655-24.

Stampley, B. E., Miller, B., Smith, R., and Scullion, T. (1995). “Pavement Management Information System Concepts, Equations, and Analysis Models. Final Report.”

Tamrakar, N. 2019. “Overview on causes of flexible pavement distresses.” 36: 6.

Tang, Z., Huang, F., and Peng, H. (2021). “Mode I Fracture Behaviors between Cement Concrete and Asphalt Concrete Layer.” *Adv. Civ. Eng.*, 2021: e6658023. Hindawi. https://doi.org/10.1155/2021/6658023.

Texas Department of Transportation. (2010). “TxDOT Research Library - Publication Details.” Accessed September 8, 2022. https://library.ctr.utexas.edu/Presto/content/Detail.aspx?ctID=UHVibGljYXRpb25fMTE2MTA=&rID=MTQ2NDU=&ssid=c2NyZWVuSURfMTg3NTU=.

Timm, D., and Turochy, R. (2014). *Pavement condition model based on automated pavement distress surveys.*

Vargas, A. (2021). “Pavement Management Systems.” Pavement Management Systems On-Demand Webinar. https://moasphalt.org/2021/pavement-management-systems-on-demand-webinar/

Vitillo, N. (2009). “Pavement Management Systems Overview.”

Wolters, A., Zimmerman, K., Schattler, K., and Rietgraf, A. (2011). *Implementing Pavement Management Systems for Local Agecies-State-of-Art/State-of-the-Practice*. llinois Center for Transportation.

Wu, G. (2015). *Development of PCI-based pavement performance model for management of road infrastructure system*. Arizona State University.

Xu, T., and Huang, X. (2012). "Investigation into causes of in-place rutting in asphalt pavement." *Constr. Build. Mater.*, 28 (1): 525–530. https://doi.org/10.1016/j.conbuildmat.2011.09.007.

Yadav, B., and Anusha, N. (2018). "Study on Phothole s." *Int. J. Eng. Technol.*, 7: 452. https://doi.org/10.14419/ijet.v7i3.34.19358.

Zhang, W., Shen, S., Basak, P., Wen, S., Faheem,W., and Mohammad, L. (2015). "Development of Predictive Models for Initiation and Propagation of Field Transverse Cracking." *Transp. Res. Rec. J. Transp. Res. Board*, 2524: 92–99. https://doi.org/10.3141/2524-09.

APPENDIX 1: ANALYSIS OF EXISTING DATABASE

The present appendix comprises a correlation analysis between the predominant distresses and the historical PCR observations (PCR from DOT) for each pavement type. The Pearson correlation coefficient was implemented as the statistical indicator to define the relation between variables. In addition, predominant distress distributions are also presented.

FLEX Pavement

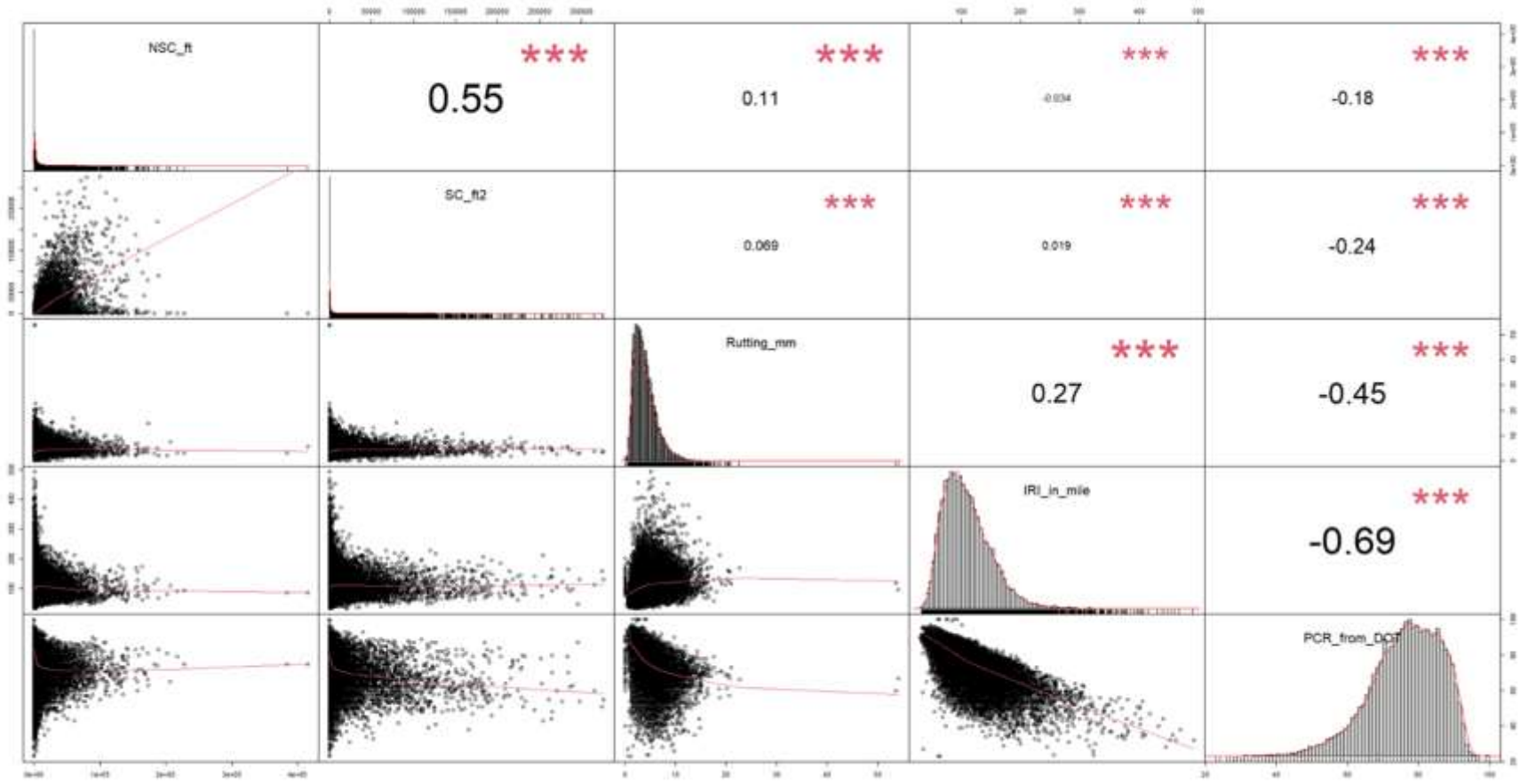

JCP Pavement

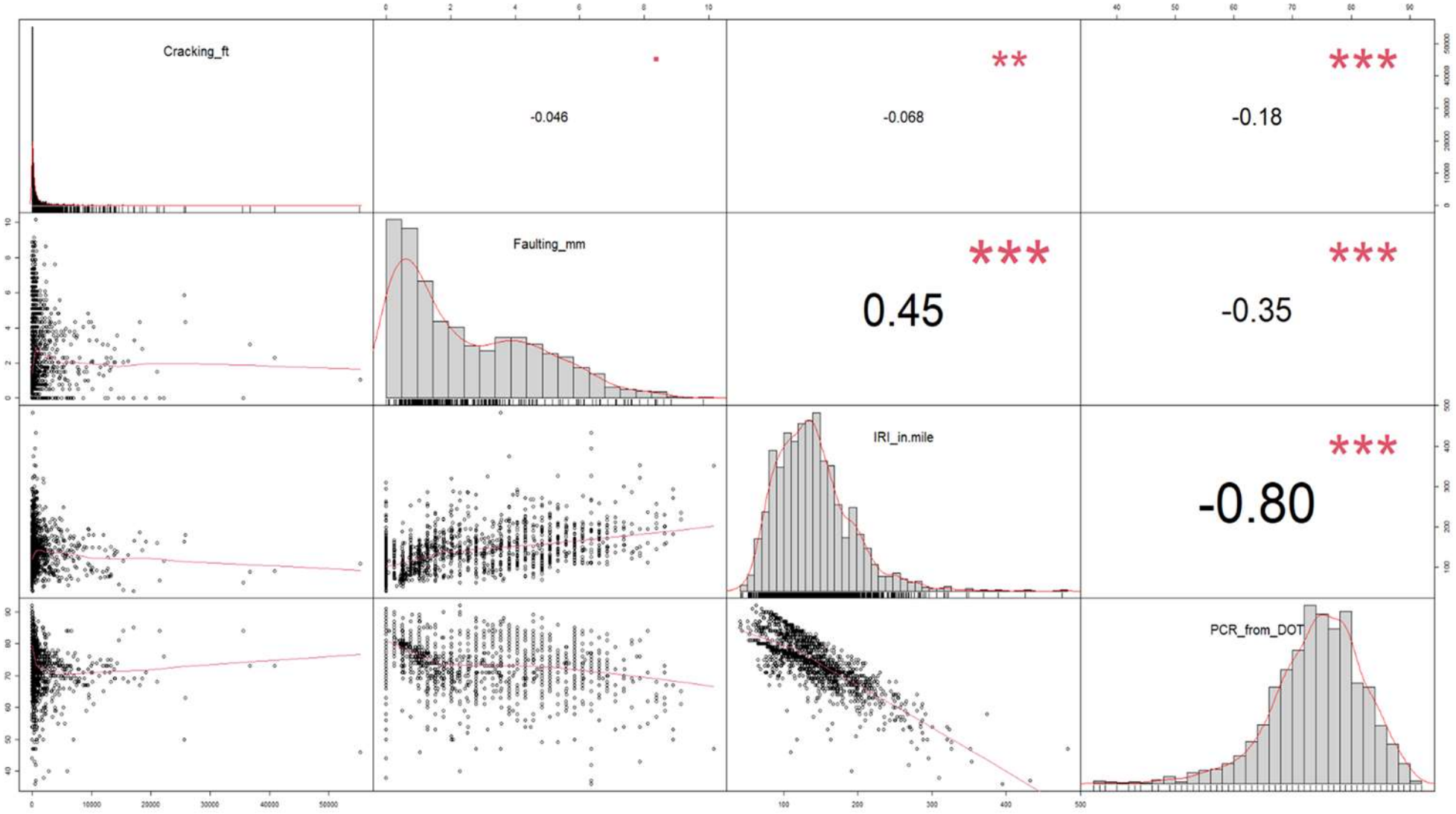

COMP Pavement

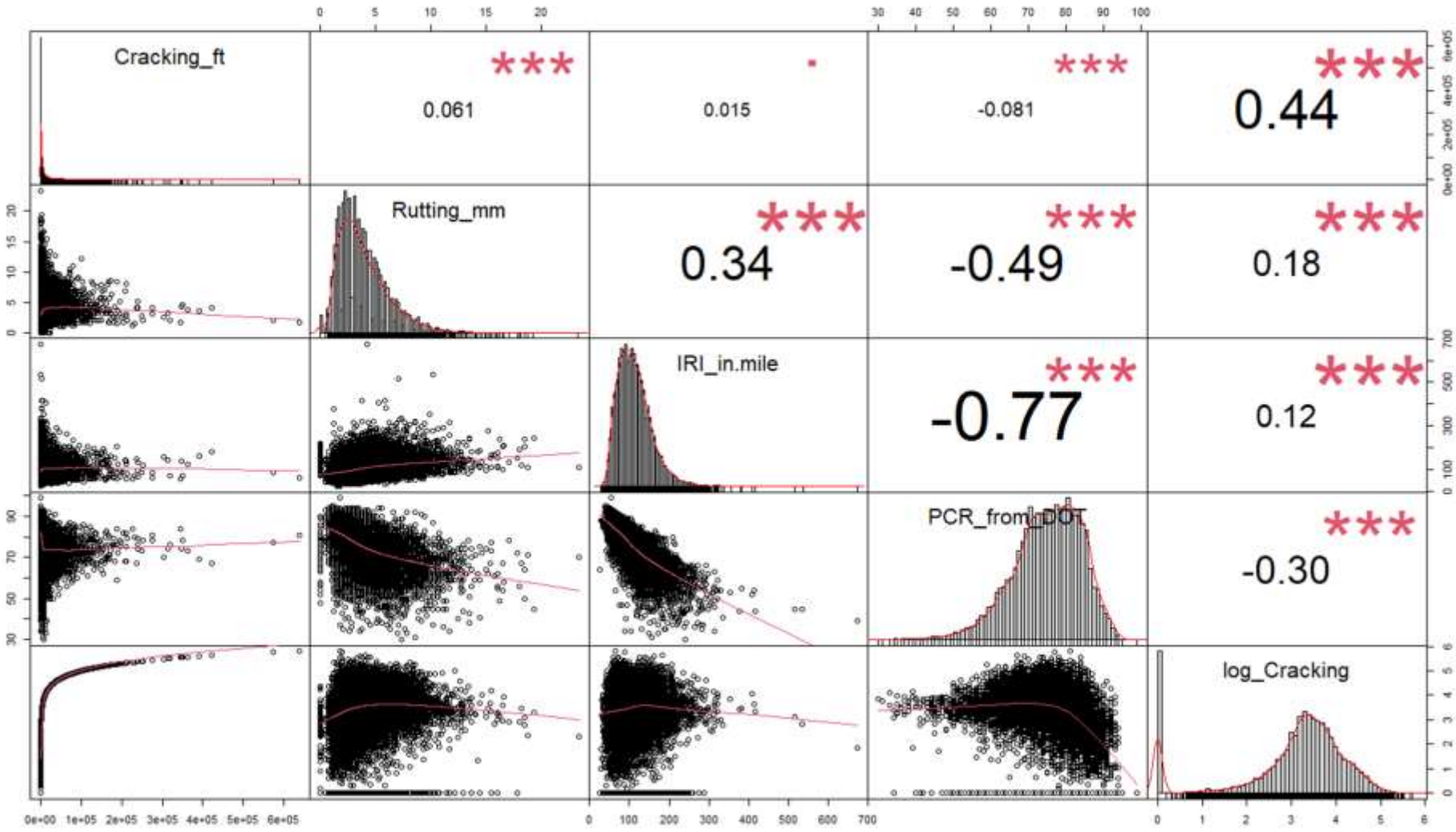

CRCP Pavement